

A dosimetric uncertainty analysis for photon-emitting brachytherapy sources: Report of AAPM Task Group No. 138 and GEC-ESTRO

Larry A. DeWerd

Department of Medical Physics and Accredited Dosimetry Calibration Laboratory, University of Wisconsin, Madison, Wisconsin 53706

Geoffrey S. Ibbott

Department of Radiation Physics, M. D. Anderson Cancer Center, Houston, Texas 77030

Ali S. Meigooni

Department of Radiation Oncology, Comprehensive Cancer Center of Nevada, Las Vegas, Nevada 89169

Michael G. Mitch

Ionizing Radiation Division, National Institute of Standards and Technology, Gaithersburg, Maryland 20899

Mark J. Rivard^{a)}

Department of Radiation Oncology, Tufts University School of Medicine, Boston, Massachusetts 02111

Kurt E. Stump

Santa Maria Radiation Oncology Center, Santa Maria, California 93454

Bruce R. Thomadsen

Departments of Medical Physics and Human Oncology, University of Wisconsin, Madison, Wisconsin 53706

Jack L. M. Venselaar

Department of Medical Physics and Engineering, Instituut Verbeeten, 5042 SB Tilburg, The Netherlands

(Received 24 June 2010; revised 6 December 2010; accepted for publication 14 December 2010; published 14 January 2011)

This report addresses uncertainties pertaining to brachytherapy single-source dosimetry preceding clinical use. The International Organization for Standardization (ISO) Guide to the Expression of Uncertainty in Measurement (GUM) and the National Institute of Standards and Technology (NIST) Technical Note 1297 are taken as reference standards for uncertainty formalism. Uncertainties in using detectors to measure or utilizing Monte Carlo methods to estimate brachytherapy dose distributions are provided with discussion of the components intrinsic to the overall dosimetric assessment. Uncertainties provided are based on published observations and cited when available. The uncertainty propagation from the primary calibration standard through transfer to the clinic for air-kerma strength is covered first. Uncertainties in each of the brachytherapy dosimetry parameters of the TG-43 formalism are then explored, ending with transfer to the clinic and recommended approaches. Dosimetric uncertainties during treatment delivery are considered briefly but are not included in the detailed analysis. For low- and high-energy brachytherapy sources of low dose rate and high dose rate, a combined dosimetric uncertainty $<5\%$ ($k=1$) is estimated, which is consistent with prior literature estimates. Recommendations are provided for clinical medical physicists, dosimetry investigators, and source and treatment planning system manufacturers. These recommendations include the use of the GUM and NIST reports, a requirement of constancy of manufacturer source design, dosimetry investigator guidelines, provision of the lowest uncertainty for patient treatment dosimetry, and the establishment of an action level based on dosimetric uncertainty. These recommendations reflect the guidance of the American Association of Physicists in Medicine (AAPM) and the Groupe Européen de Curiethérapie–European Society for Therapeutic Radiology and Oncology (GEC-ESTRO) for their members and may also be used as guidance to manufacturers and regulatory agencies in developing good manufacturing practices for sources used in routine clinical treatments. © 2011 American Association of Physicists in Medicine.

[DOI: 10.1118/1.3533720]

Key words: brachytherapy, dosimetry, uncertainty, standards

TABLE OF CONTENTS

I. INTRODUCTION.....	783	III. MEASUREMENT UNCERTAINTY IN BRACHYTHERAPY DOSIMETRY.....	785
II. UNCERTAINTY ESTIMATION METHODS.....	784	III.A. Intrinsic measurement uncertainties.....	785
		III.A.1. Source activity distribution.....	785
		III.A.2. Source-to-detector positioning.....	785

III.B. Dose measurement.	786
III.B.1. Thermoluminescent dosimeters.	786
III.B.2. Radiochromic film.	786
III.B.3. Diamonds, diodes, and MOSFETs.	787
IV. MONTE CARLO UNCERTAINTY IN BRACHYTHERAPY DOSIMETRY.	787
IV.A. Source construction.	787
IV.B. Movable components.	788
IV.C. Source emissions.	788
IV.D. Phantom geometry.	789
IV.E. Phantom composition.	789
IV.F. Radiation transport code.	789
IV.G. Interaction and scoring cross sections.	790
IV.H. Scoring algorithms and uncertainties.	790
V. UNCERTAINTY IN THE TG-43 DOSIMETRY FORMALISM PARAMETERS.	790
V.A. Air-kerma strength.	790
V.A.1. Uncertainty in NIST primary standard for LDR low-energy photon-emitting sources.	790
V.A.2. Uncertainty in NIST primary standard for LDR high-energy photon-emitting sources.	791
V.A.3. S_K uncertainty for HDR high-energy sources.	791
V.A.4. Transfer of NIST standard to the ADCLs.	792
V.A.5. Transfer of NIST standard from ADCLs to the clinic.	792
V.B. Dose-rate constant.	794
V.C. Geometry function.	794
V.D. Radial dose function.	795
V.E. 2D anisotropy function.	795
V.F. 1D anisotropy function.	795
V.G. TPS uncertainties summary.	795
VI. RECOMMENDATIONS.	796
VI.A. General uncertainty.	796
VI.B. Clinical medical physicists.	796
VI.B.1. S_K and TPS data entry.	796
VI.B.2. Treatment planning system developments.	796
VI.B.3. Clinical dosimetric uncertainties.	797
VI.C. Dosimetry investigators.	797
VI.D. Source and TPS manufacturers.	798
VII. SUMMARY AND COMPARISON TO EXISTING WRITTEN STANDARDS.	798

I. INTRODUCTION

This report addresses uncertainties pertaining to photon-emitting brachytherapy source calibrations and source dosimetry. In the American Association of Physicists in Medicine (AAPM) TG-40 report,¹ the desired level of accuracy and precision is provided for treatment delivery. It is generally assumed that brachytherapy uncertainties are larger than those in external beam applications. One objective of the current report is to quantify the uncertainties involved in brachytherapy so a greater understanding can be achieved. The uncertainty values of brachytherapy apply to both the experimentally measured and Monte Carlo (MC)-estimated

values. The 2004 AAPM TG-43U1 report considered these uncertainties in a cursory manner.² Before publication of the TG-43U1 report, estimates of dosimetry uncertainties for brachytherapy were limited. Most investigators using MC techniques presented only statistical uncertainties; only recently have other MC uncertainties been examined.

In the current report, the uncertainty propagation from the primary calibration standard through transfer to the clinic for air-kerma strength S_K is detailed (Fig. 1). Uncertainties in each of the brachytherapy dosimetry parameters are then explored, and the related uncertainty in applying these parameters to a TPS for dose calculation is discussed. Finally, recommended approaches are given. Section II contains detailed explanations of type A and type B uncertainties. The brachytherapy dosimetry formalism outlined in the AAPM TG-43 report series [1995,³ 2004,² and 2007 (Ref. 4)] is based on limited explanation of the uncertainties involved in the measurements or calculations. The 2004 AAPM TG-43U1 report presented a generic uncertainty analysis specific to calculations of brachytherapy dose distributions. This analysis included dose estimations based on simulations using experimental measurements using thermoluminescent dosimeters (TLDs) and MC methods. These measurement and simulation uncertainty analyses included components toward developing an uncertainty budget. A coverage factor of 2 ($k=2$) is recommended for testing and calibration laboratories per the International Organization for Standardization (ISO) 17025 report⁵ and in general for medicine;⁶ we also recommend this coverage factor for the scope of uncertainties included in the current report. Thus, a coverage factor of 2 is used in the current report unless explicitly described otherwise.

The current report is restricted to the determination of dose to water in water without consideration of material heterogeneities, interseed attenuation, patient scatter conditions, or other clinically relevant advancements upon the AAPM TG-43 dose calculation formalism.⁷ Specific commercial equipment, instruments, and materials are described in the current report to more fully illustrate the necessary experimental procedures. Such identification does not imply recommendation or endorsement by either the AAPM, ESTRO, or the U.S. National Institute of Standards and Technology (NIST), nor does it imply that the material or equipment identified is necessarily the best available for these purposes. These recommendations reflect the guidance of the AAPM and GEC-ESTRO for their members and may also be used as guidance to manufacturers and regulatory agencies in developing good manufacturing practices for sources used in routine clinical treatments. As these recommendations are made jointly by the AAPM and ESTRO standing brachytherapy committee, the GEC-ESTRO, some of the specifically mentioned U.S. agencies, organizations, and standard laboratories should be interpreted in the context of the arrangements in other countries where applicable. In particular, other primary standards laboratories, such as the Physikalisch-Technische Bundesanstalt (PTB) in Braunschweig, Germany, the National Physical Laboratory (NPL) in the United Kingdom, and the Laboratoire National Henri

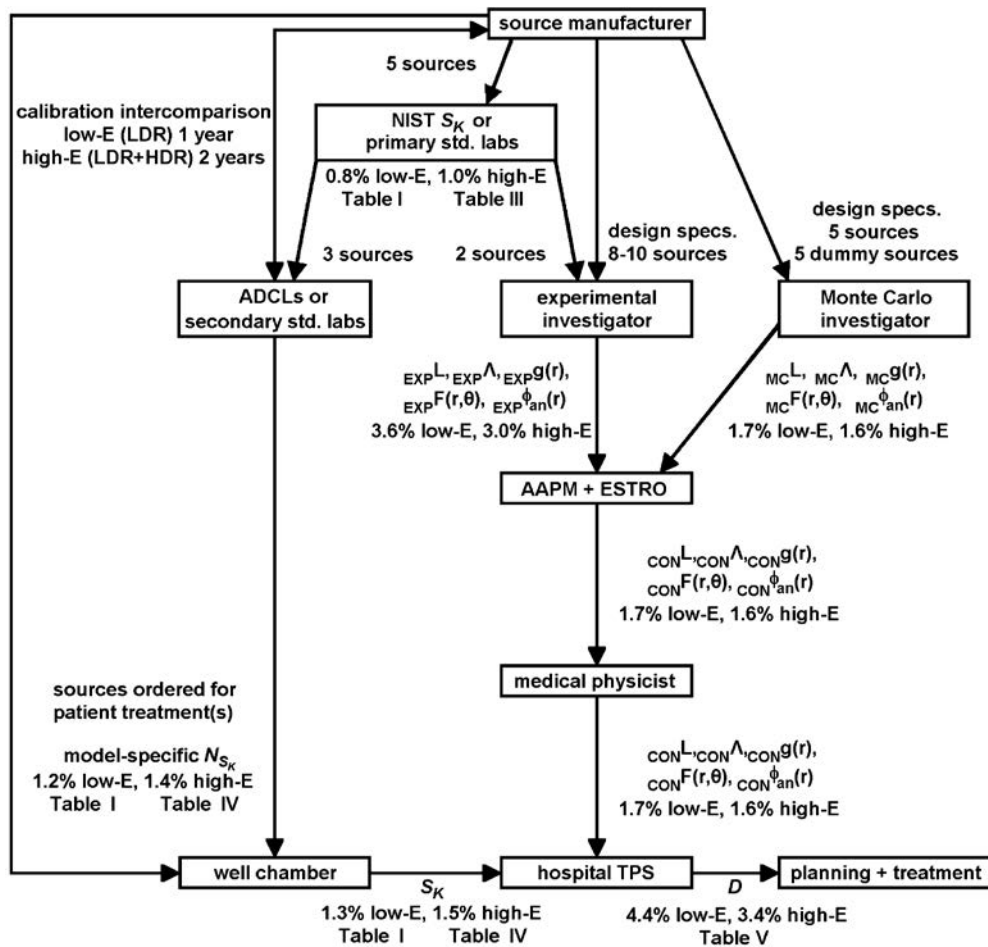


FIG. 1. Brachytherapy source dosimetry data chain, highlighting the uncertainty values ($k=1$) and how they combine to increase the overall dosimetric uncertainty for the U.S. The low- E and high- E refer to low- and high-energy photon-emitting sources, respectively, and are representative of both LDR and HDR brachytherapy sources. The symbols and notation in this figure are in accordance with the 2004 AAPM TG-43U1 report. Symbols such as EXP^L , MC^L , and CON^L represent the active lengths used by the experimental investigators, Monte Carlo simulation investigators, and the consensus value, respectively. Following the flow chart, manufacturers first create sources and follow the AAPM 2004 CLA subcommittee recommendations for initial source calibrations by sending sources to a primary standards laboratory (e.g., NIST) then to the secondary standards laboratories (e.g., ADCLs) and experimental dosimetry investigator(s). The AAPM and GEC-ESTRO then prepare candidate and consensus dosimetry parameters to serve as reference datasets for widespread and uniform clinical implementation. Clinical medical physicists should use these data whenever available and assure proper entry and QA for commissioning in their TPS. At the upper-left, calibration intercomparisons are performed to ensure manufacturers are in agreement with the primary and secondary standards laboratories. When the clinical medical physicist orders sources for treating a patient, sources are calibrated on site using equipment calibrated at a secondary standards laboratory or ADCL with direct traceability to a primary standards laboratory (e.g., NIST) according to AAPM 2008 LEBSC recommendations. The patient-specific source strength S_K is entered into the TPS, and clinical treatment planning and treatment delivery are performed.

Becquerel (LNHB) in France perform brachytherapy source calibrations, each measurement system having an associated uncertainty budget. It should be noted that many of these uncertainties affect source parameters before use in the clinic and the clinical medical physicist has no control over them.

II. UNCERTAINTY ESTIMATION METHODS

Uncertainty is a useful and important concept for quantitatively determining the accuracy of measurements and calculations. Uncertainty analysis is different from the outdated method of random and systematic errors. The terms *accuracy* and *precision* are still maintained but with slightly different definitions. Accuracy is defined as the proximity of the result to the conventional true value (albeit unknown) and is an indication of the correctness of the result. Precision is de-

finied as a measure of the reproducibility of the result. A stable instrument capable of making high-precision measurements is desired since it can be calibrated to provide an accurate result. Uncertainty determination takes into account measurement or calculation variations, including all of the precisions of the measurements or calculations and their effects on the results. Thus, uncertainty is a part of every measurement or calculation. The hardest part of uncertainty determination is to account for all possible influences. The uncertainty can be thought of as a defining interval, which is believed to contain the true value of a quantity with a certain level of confidence. For a coverage factor of 2 (see above), the true value of the quantity is believed to lie within the uncertainty interval with a 95% level of confidence.

The present-day approach to evaluating uncertainty in

measurements is based on that recommended by the Comité International des Poids et Mesures (CIPM) in 1981.⁸ The CIPM recommendations included grouping uncertainties into two categories (type A and type B, to be explained below), as well as the methods used to combine uncertainty components. This brief CIPM document was expanded by an ISO working group into the *Guide to the Expression of Uncertainty in Measurement* (GUM), first published in 1993 and subsequently updated in 2010.⁹ This formal method of assessing, evaluating, and reporting uncertainties in measurements was presented in a succinct fashion in NIST Technical Note 1297, *Guidelines for Evaluating and Expressing the Uncertainty of NIST Measurement Results* (1994).¹⁰ The main points of this Technical Note relevant to the current report are summarized below.

Components of measurement uncertainty may be classified into two types, namely, those evaluated by statistical methods (type A) and those evaluated by other means (type B). In the past, type A and type B uncertainties were commonly referred to as *random* and *systematic* errors (more properly uncertainties), respectively. The use of the term *error* is discouraged in uncertainty analyses since it implies a mistake or refers to the difference between the measured value of a quantity and the true value, which is unknown. For example, what might be considered as an error by one dosimetry investigator could be considered an uncertainty by another investigator. Specifically, investigator 1 might assign a large uncertainty to the dimensions of internal source components without having first-hand knowledge of source construction or the ability to open the capsule. Investigator 2 might question the values used by investigator 1, considering them erroneous, having opened the capsule and measured the dimensions of the internal components. If the true value was known, there would be no need to perform the measurement.

Representing each component of uncertainty by an estimated standard deviation yields the *standard uncertainty*, u . For the i th type A component, $u_i = s_i$, the statistically estimated standard deviation is evaluated as the standard deviation of the mean of a series of measurements. For the j th type B component, u_j is an estimate of the corresponding standard deviation of an assumed probability distribution (e.g., normal, rectangular, or triangular) based on scientific judgment, experience with instrument behavior, and/or the instrument manufacturer's specifications. Historical data in the form of control charts from a given measurement process may be used to evaluate type B components of uncertainty. The *combined standard uncertainty* u_c represents the estimated standard deviation of a measurement result and is calculated by taking the square root of the sum-of-the-squares of the type A and type B components. This technique of combining components of uncertainty, including relevant equations such as the Law of Propagation of Uncertainty, is illustrated in Sec. IV C of the TG-43U1 report.² In the current report, uncertainty propagation is accomplished by adding in quadrature the relative (%) uncertainties at each step of a measurement traceability chain. This is only the case since the measurement equation is a simple product of measured or calculated quantities. If the probability distribution

characterized by the measurement result y is approximately normal, then $y \pm u_c$ gives an interval within which the true value is believed to lie with a 68% level of confidence.

Normally, the symbol U is used to express the *expanded uncertainty*; however, to avoid confusion with the unit U for air-kerma strength, this AAPM/GEC-ESTRO report uses the symbol V for this quantity. An expanded uncertainty $V = k u_c$, where k is the coverage factor, is typically reported and is applied only to the combined uncertainty, not at each stage of an evaluation. Assuming an approximately normal distribution, $V = 2 u_c$ ($k = 2$) defines an interval with a 95% level of confidence, and $V = 3 u_c$ ($k = 3$) defines an interval with a level of confidence $> 99\%$. When there is limited data and thus u_c has few degrees of freedom, $k = t$ factor is determined from the t distribution.^{9,10}

III. MEASUREMENT UNCERTAINTY IN BRACHYTHERAPY DOSIMETRY

There are a number of uncertainties involved in brachytherapy dosimetry measurements. These measurements are usually performed at research facilities outside the clinic. Dosimetry investigators should propose methods to quantify all these uncertainties and specify them in their publications.

III.A. Intrinsic measurement uncertainties

Inherent characteristics of the source and devices used for dosimetric measurements include knowledge of the source activity distribution and source-to-detector positioning. These characteristics contribute to dosimetric uncertainties, often specific to the model of source and detector.

III.A.1. Source activity distribution

An uncertainty in source activity distribution on the internal substrate components becomes a systematic uncertainty, propagating to all dosimetric measurements. Most brachytherapy sources are assumed to be uniform about the circumference of the long axis due to their cylindrical symmetry. However, in reality the vast majority of sources demonstrate variations of 2%–20% in the intensity of emissions about the long axis for high- and low-energy photon emitters. Such variations are reflected in the statistical uncertainty of measurements if measurements are made at numerous circumferential positions around the source, and the results are averaged.^{11,12} These variations have been demonstrated in calibrations performed at NIST.¹³

III.A.2. Source-to-detector positioning

Several types of uncertainty arise from the relative positions of the source and detector and depend on the phantom material and the detector. If TLDs are used, the detector shape (rods, chips, or capsules of powder) may lead to different uncertainties in the location of the detector relative to the source. Film, generally radiochromic film, has become a common detector for brachytherapy dose measurements. The positional uncertainty for film has two components: the positioning of the film and the positional uncertainty for relat-

ing the reading of the optical density to the position in the phantom. For measurements of some parameters, such as dose-rate constant Λ and radial dose function $g(r)$, the source is positioned normal to the detector plane. A type A dosimetric uncertainty in detector distance from the source relative to the mean detector distance appears as an uncertainty in detector reading. However, a type B uncertainty in the mean distance of a group of detectors must be considered in the analysis of Λ and $g(r)$. For measurements of the 2D anisotropy function $F(r, \theta)$, the uncertainty in the distance of each detector from the source must be determined. In addition, the uncertainty in the angle from the source long axis must be considered. Taylor *et al.*¹⁴ determined the uncertainty ($k=1$) in the mean distance to the detectors in a water phantom to be 0.09 mm. However, Taylor *et al.*¹⁵ claimed a seed-to-TLD positioning uncertainty of 0.05 mm ($k=3$) for a 0.3% type B component dosimetric uncertainty at $r=1$ cm. More typical values obtained by a routine investigator would fall around 0.5 mm ($k=1$).

The uncertainty in the detector point of measurement varies somewhat with the phantom material and related technique. If a water tank scanner is used, there is an uncertainty associated with the movement and positioning. A scanning system might display a source-to-detector positioning precision of 0.1 mm. However, typical positioning accuracy of a water tank scanner is about 0.4 mm, expressed as $k=2$.¹⁶ The accuracy is more difficult to specify, in part, because of the uncertainty in the source-positioning device and also because of the uncertainty in the effective point of measurement for the detector. Considering only the effects of geometry (i.e., the inverse-square relationship) and ignoring signal variation across the detector (i.e., a pointlike detector), the dosimetric effects of a 0.04 cm positional uncertainty at distances of 1 cm and 5 cm are 8% and 1.6%, respectively.

For dose rate measurements of the same duration at these positions, the reading at 5 cm is 25 times lower than the 1 cm reading due to the inverse-square effect alone, not accounting for medium attenuation. For measurements involving low-energy photon emitters, the relative signal at the greater distance is considerably lower due to medium attenuation that is not compensated by increased scatter. Most often, the detectors used for brachytherapy dosimetry measurements are not limited by counting statistics, but rather intrinsic properties such as signal-to-noise ratio and detector reproducibility. This often produces an uncertainty at 5 cm about ten times larger than that at 1 cm. When compared to source-to-detector positioning uncertainty, there is partial compensation between these two effects. The decreased signal with distance can sometimes be overcome when using integrating dosimeters simply by leaving the dosimeters in place for a longer time. Radionuclides with short half-lives limit the improvement that can be achieved by increasing the exposure duration. For ¹⁰³Pd, with a 17-day half-life, the dose rate at 5 cm is only 0.4% of that at 1 cm in water. To obtain 1 Gy at 1 cm from a 1 U source requires about 6.9 days. At 5 cm from this same source, the maximum dose possible after

complete decay of the source is less than 1.5 cGy. Thus, extending the exposure time for the more distant points cannot be considered equivalent.

III.B. Dose measurement

There are unique challenges to measuring radiation dose in the presence of either a high dose gradient or a very low dose rate (LDR), particularly for low-energy photon-emitting sources. The major consideration is the need for a detector with a wide dynamic range, flat energy response, small geometric dimensions, and adequate sensitivity. Radiation measurement devices in general use for brachytherapy source dosimetry are LiF TLDs, radiochromic films, diamond, diode, and metal-oxide-field effect transistor (MOSFET) detectors. These detector types are considered below and may be chosen for their dynamic dose range, high-spatial resolution, feasibility for *in vivo* dosimetry, approximation to human soft tissue, or relative ease of use. However, the accuracy of the results from these detectors is subject to the uncertainties due to volume averaging, self-attenuation, and absorbed-dose sensitivity. At the small source:detector distances of brachytherapy, detector size can influence self-attenuation and volume averaging.

III.B.1. Thermoluminescent dosimeters

TLDs have been the main dosimeter used for measurement of brachytherapy source dose. Typically, these measurements have been made in solid-water phantoms comprised of plastics having radiological characteristics similar to water. Kron *et al.*¹⁷ provided characteristics that should be reported each time a TLD measurement is made. A calibration of the TLDs to a known energy and dose is necessary to perform dosimetry. Two major sources of uncertainty are the annealing regime used by different investigators and the intrinsic energy dependence $k_{Bq}(Q)$, which is per unit of activity (i.e., Becquerel). Depending on the temperatures and cooling for the materials, the uncertainty can increase drastically, from 1% to 5%. The uncertainty is reduced when meticulous care is used in the handling, reading, and irradiation conditions. The other large source of uncertainty is the variation in the TLD absorbed-dose sensitivity between the energy used for calibration and that of the brachytherapy source. This is the uncertainty in the relation of the energy dependence of the absorbed-dose sensitivity relative to that in the beam quality used for calibration. Each reading regime should be the same to reduce the variation. The characteristics that affect thermoluminescence are elaborated upon in Chap. 24 of the 2009 AAPM Summer School text.¹⁸ If care is taken in each of the regimes, an overall estimate of the expanded uncertainty to measure absorbed dose would be 5.58% ($k=2$).¹⁹

III.B.2. Radiochromic film

Radiochromic film has become a common detector for brachytherapy measurements. Advantages of EBT film compared to silver halide film include the following: relative

energy insensitivity, insensitivity to visible light, self-developing characteristics, greater tissue equivalency, and dose-rate independence.^{20–23} Different investigators have noted up to 15% variation in the film response throughout a film that was exposed to a uniform dose of radiation. Sources for these uncertainties have been pointed out by Bouchard *et al.*²⁴ Looking at two orthogonal directions, the film response is more uniform in one direction. Applications of various models of radiochromic film in radiation dosimetry have been discussed in detail in AAPM TG-55 (Ref. 25) and more recently by Soares *et al.*²⁶ Radiochromic film response is independent of dose rates in the clinical range of 0.1–4 Gy/min. Dini *et al.*²³ showed that the responses of both XR type T and type R films were independent of the dose rate. The results of their investigations showed a 5% variation for dose rates ranging from 0.16 to 7.55 Gy/min. These results were in good agreement with the finding of Giles and Murphy,²⁷ who had shown that XR type films are dose-rate-independent within 5%. In an independent investigation, Saylor *et al.*²¹ showed 5% variation in optical densities of HD-810 film for dose rates ranging from 0.02 to 200 Gy/min. However, many of the reports in the literature pertain to older films that are not useful for current brachytherapy measurements. The manufacturer discontinued production of EBT film and now only provides the EBT2 model. The dosimetric uncertainties of brachytherapy source measurements made with EBT2 are increasingly being investigated.^{28–30} Before use, the dosimetry investigator should be aware of the characteristics of the individual type of film.

In general, the handling of the film can be important so that exposure to ultraviolet light and other conditions are minimized; again the uncertainty can be reduced if this care is taken. An estimate of the expanded uncertainty to measure absorbed dose is 10%.^{30,31} Due to the increasing number of different radiochromic films and their dependence on scanning techniques, caution is recommended. In addition, it is important to realize that the scanner can have a significant effect on the results of the film.³² While investigations have been made for various scanners such as by Hupe and Brunzendorf³¹ and by Alva *et al.*,³³ there have been conflicting results requiring further research.

III.B.3. Diamonds, diodes, and MOSFETs

Occasionally, measurements in a water phantom use diode or diamond detectors, but their dosimetric uncertainties can exceed 15% ($k=1$) for low-energy photon-emitting brachytherapy sources.³⁴ These uncertainties result from the large energy dependence of its absorbed-dose sensitivity, nonlinearity, directional dependence, temperature dependence, and bias dependence, especially when used for low-energy brachytherapy sources. Diode characteristics are given in the AAPM TG-62 report by Yorke *et al.*³⁵ MOSFET dose response is also energy and dose-rate dependent.^{36,37} While MOSFETs have been used for brachytherapy *in vivo* dosimetry,^{38,39} they have not been used to date for direct dosimetric parametrization of brachytherapy sources.

IV. MONTE CARLO UNCERTAINTY IN BRACHYTHERAPY DOSIMETRY

While MC methods may be used to characterize brachytherapy source dosimetry accurately, there are both obvious and hidden uncertainties associated with the process that must be accounted for. For large numbers of histories where Poisson statistics applies, the uncertainty in the estimated results decrease by the inverse square root of the number of particle histories. This uncertainty is referred to as the type A uncertainty for MC methods and should be kept to <0.1% when feasible so as to be negligible in comparison to other computational uncertainties. In many cases, it is unfeasible to simulate additional histories due to processing power and time constraints. While variance reduction techniques are sometimes used to diminish type A uncertainties, careful benchmarking is required for radiation transport codes and their individual features and subroutines. The MC dosimetric uncertainty analysis presented in Table XII of the TG-43U1 report listed four separate components² and has been substantially expanded here into eight separate components (all but one being type B). These roughly correspond chronologically (for nonadjoint particle transport) with the MC simulation process and must be estimated by each dosimetry investigator for the specific source and circumstance being studied. Consequently, example tables are not provided since the results are dependent on the energy of the source emissions, capsule design, simulation goals, and MC code. This subsection reviews the simulation process and current state-of-the-art for uncertainty analyses. It is important to clarify the methods used to arrive at values for the dosimetric component uncertainties and aspire to minimize these uncertainties. Manufactured sources may differ from their design; MC simulations should be performed with representations of the final clinically delivered product. What follows are descriptions of uncertainties that arise throughout the process of using MC methods to simulate dose-rate distributions in the vicinity of brachytherapy sources. Dosimetry investigators are urged to consider these analyses and introduce detailed estimates in future brachytherapy dosimetry publications.

IV.A. Source construction

Characterization of brachytherapy dose-rate distributions starts with a full understanding of the source construction. In general, brachytherapy sources contain radionuclides that are sealed in a single capsule. High dose-rate (HDR) sources have the capsule attached to a delivery cable used to position the individual source at multiple locations within the patient. Pulsed dose-rate sources are similar to HDR, but the treatment is applied in a protracted manner. LDR sources may be described as individual entities and do not utilize a delivery cable. However, they may be contained within metal or plastic cylinders or a surgical suture material as is the case for stranded seeds. With the current TG-43 dosimetry formalism for low-energy sources based on superposition of individual sources within a 30 cm diameter water phantom to provide full-scatter conditions for $r \leq 10$ cm, all that is required is characterization of the active radionuclide and the source.²

The dosimetry investigator should independently assess available manufacturer data on source construction, estimate the uncertainties associated with each dimension, and estimate the distribution of results within the available range of results. A theoretical example is provided for how to characterize the source geometry uncertainties for a hypothetical brachytherapy source.

- (a) The capsule is a right cylinder made of pure (100%) titanium ($\rho=4.51 \pm 0.05 \text{ g/cm}^3$), with inner and outer diameters of 0.70 and 0.80 mm (rectangular distribution over a tolerance of $\pm 0.02 \text{ mm}$), respectively, overall length of 4.52 mm (rectangular distribution over a tolerance of $\pm 0.05 \text{ mm}$), and end-weld thicknesses of 0.15 mm (rectangular distribution over a tolerance of $\pm 0.03 \text{ mm}$).
- (b) The capsule is filled with room temperature Ar gas ($\rho=1.78 \pm 0.04 \text{ mg/cm}^3$) and an Ir pellet.
- (c) The Ir source pellet ($\rho=22.56 \pm 0.01 \text{ g/cm}^3$) is a right cylinder with a 0.66 mm diameter (rectangular distribution over a tolerance of $\pm 0.01 \text{ mm}$) and 4.10 mm active length L (rectangular distribution over a tolerance of $\pm 0.02 \text{ mm}$) with a ^{192}Ir loading of $(3.2 \pm 0.2) \times 10^{11}$ atoms uniformly distributed throughout the pellet.

This description presents $k=1$ uncertainties associated only with capsule dimensions, internal components, and location of radiation emission. A sophisticated MC dosimetric analysis would simulate the influence of varying each of these components and estimate the resultant effect of these uncertainties on the calculated dose distribution. Karaikos *et al.*⁴⁰ investigated the effect of varying the silver halide coating thickness (i.e., 1–10 μm) for an ^{125}I source; Λ and $g(r)$ were unchanged within 1%. Koona⁴¹ assessed variable ^{125}I source capsule wall thickness (i.e., 30–100 μm) and found an influence on Λ ranging from +16% to –1%. For similar endweld thicknesses, differences in Λ ranged from –0.2% to 0.9%. However, the variation in the endweld thickness led to a significant impact on $F(r, \theta)$ for small polar angles.

IV.B. Movable components

As shown by Rivard, the internal components within the capsule may change position.⁴² The dimensions from source to source may vary also. At distances of a few millimeters from some sources, the dose rate can change more than a factor of 2 upon varying the capsule orientation.⁴² Since most low-energy sources do not have their internal components rigidly attached to the encapsulation, it is possible that the internal components may move about based on the source orientation. Especially for a low-energy photon-emitting source containing radio-opaque markers for localization, such dynamic aspects may be of clinical relevance under certain circumstances. While this effect can be observed experimentally when the source orientation is rotated 180°, this behavior is readily assessable using MC methods, but more challenging with experimental techniques where localization of the internal components may be unknown. To

ascribe MC dosimetric uncertainties to this component, the full range of motion should be considered, along with possibilities for configuring internal components if multiple items are free to move and subtend different geometries upon settling within the capsule. An example is provided.

- (a) For the example given in the source geometry uncertainty description, the Ir pellet could move $\pm 0.25 \text{ mm}$ along the capsule long axis and $\pm 0.035 \text{ mm}$ in the lateral direction within the capsule due to a combination of dimensional tolerances.
- (b) In addition to the aforementioned shifts, the pellet could possibly rotate within the capsule.

Clearly, the single internal component (Ir pellet) is well constrained, and dosimetric uncertainties due to a dynamic internal component would be small compared to other dosimetric uncertainty components. However, this would not be the case if the internal component containing a low-energy photon-emitting radionuclide were much smaller and nestled behind a radio-opaque marker where the radiation emissions would be substantially attenuated in comparison to an optimized geometry for the internal components.

It appears that the dynamic internal components of sources can have the largest influence on dose rate variations and thus should be considered for the source models, positions of interest, and source orientation relevant to the clinical application. In general, the dosimetric uncertainty related to internal component movement increases as photon energy decreases. While not an important aspect for all sources, the dosimetry investigator should assess the impact of this effect for the type of source being examined since some sources are fairly susceptible to this effect (previously mentioned factor of 2) where other sources exhibit less than a 0.1% dosimetric effect at the reference position.⁴³ Time-averaged internal component positions should be used for reference data, and the dosimetric uncertainties for all possible internal component positions should be considered.

IV.C. Source emissions

Brachytherapy sources generally contain radioactive materials and have capsules to prevent direct contact of the radioactive materials with patients. Exceptions include electronic brachytherapy sources, which generate radiation without radionuclides,^{44,45} and the ^{103}Pd RadioCoil source.⁴⁶ Since nuclear disintegration processes are well understood, there is little uncertainty associated with knowledge of the radiation spectrum from the radioactive materials. A general uncertainty in dose rate per unit source strength at $P(r_0, \theta_0)$ of 0.1% for low-energy sources⁴³ and 0.5% for high-energy sources⁴⁷ may be assumed. However, physical fabrication of brachytherapy sources often involves radiochemistry and other processes to purify the isotopic and elemental composition of the radioactive product. With radiocontaminants having different half-lives than the desired radionuclide, there may be substantial uncertainty concerning the radionuclides contained in the source. When simulated using MC methods, the dosimetry investigator is advised not to assume

a pure radioactive product and to include the contaminant radionuclides and daughter products in the carrier material if the presence of such contaminants has been verified (mass-spectroscopy measurements and/or photon spectrometry measurements). Further, electron dose contributions from sources generally considered as photon emitters should be considered.^{48–50}

The National Nuclear Data Center (NNDC) at Brookhaven National Laboratory is an internationally regarded reference for radionuclide radiation spectra.⁵¹ This database includes all of the commonly used radionuclides in brachytherapy, often listing the precision of photon and electron energies to four significant digits and the emission intensities to three significant digits and probabilities to parts per million. As a result of uncertainties in the source photon energies and the exaggerated precision of emission probabilities, the dosimetry investigator should consider the influence of an inaccurate spectral characterization on the resultant dose distribution. This latter feature would be most meaningful for considering relatively new radionuclides, sources with novel means of generating radiation, and sources that contain radionuclides which emit both photons and electrons.

IV.D. Phantom geometry

Phantom size has a significant effect on brachytherapy dose distributions.^{52–54} Although variations in radiation scatter and attenuation are readily accounted for with modern external-beam TPS, brachytherapy TPS generate dosimetry data based on brachytherapy dosimetry parameters and may not account for full-scatter conditions or appropriate scatter conditions for the task at hand. Thus, the dosimetry investigator should describe the phantom size used in the simulations and should estimate the influence of scatter conditions over the positions in which dose was calculated. The current brachytherapy dosimetry formalism,² based on the AAPM TG-43 report,³ stipulates that MC calculations be performed in a 15 cm radius liquid water phantom to provide at least 5.0 cm of radiation backscatter for low-energy photon-emitting sources such as ¹²⁵I and ¹⁰³Pd at the farthest position from the source. By the current AAPM definition, low-energy photon-emitting sources are those which emit photons of energy less than or equal to 50 keV.² Under these circumstances for a 50 keV photon-emitting source, approximately 5.0 and 7.5 cm of backscattering material are needed to simulate infinite scatter conditions within 3% and 1%, respectively.⁵³ Thus, the initially recommended 5.0 cm of backscatter to simulate infinite scatter conditions within 1% applies only for photon-emitting sources with $E < 40$ keV.

IV.E. Phantom composition

Presently, the TG-43 dosimetry formalism does not account for material heterogeneities and recommends liquid water as the reference media for specification of *in vivo* dose-rate distributions. Being a simple and readily available material, it is not challenging to simulate the composition (H₂O) and mass density ($\rho = 0.998$ g/cm³ at 22 °C) of liquid water. However, care must be taken when the dosimetry

investigator aims to simulate the geometry of a physical experiment. Here, the setup will often include a plastic medium in place of liquid water. Due to the variable nature in fabricating these plastic media, the dosimetry investigator is advised to determine the composition and mass density independently and assign uncertainties to this assessment. Furthermore, these uncertainties directly impact the resultant dosimetric uncertainties, which should be assigned to the phantom composition. In contrast to phantom size, the MC dosimetric uncertainties due to phantom composition generally increase with decreasing photon energy and increase with increasing radial distance.

Specification of a solid phantom material is important for dosimetric evaluation of brachytherapy sources, particularly for low-energy photon-emitting sources.^{16,55} Meigooni *et al.*⁵⁵ showed that a 0.4% difference in the calcium content of the Solid Water™ phantom material may lead to 5% and 9% differences in Λ for ¹²⁵I and ¹⁰³Pd sources, respectively. These results are in good agreement with the published data by Patel *et al.*,⁵⁶ who performed a robust material analysis of the phantom composition. In addition, Meigooni *et al.* showed the impact of the phantom composition on $g(r)$ for both ¹²⁵I and ¹⁰³Pd sources.⁵⁵ Small differences in phantom composition lead to large differences in $g(r)$ for low-energy photon emitters. Differences were more significant at larger depths from the source, and they concluded that one must use updated correction factors based on correct chemical composition and cross-section data when extracting a consensus of dosimetric parameters for a brachytherapy source by means of the TG-43U1 protocol.² Dosimetric uncertainties arising from uncertainties in phantom composition are typically classified as type B.

IV.F. Radiation transport code

All MC codes use approximations and assumptions when simulating radiological interactions. For example, generation of multiple-photon emissions following characteristic x-ray production may be simplified to the most probable photons, some MC codes ignore electron binding effects, and electron transport is often reduced to a multigroup algorithm or ignored entirely. Although molecular form factors can be used in some codes, there is no significant dosimetric effect when using an independent-atom approximation for coherent scattering form factors.⁵⁴ Specific to the use of radiation transport codes for determining brachytherapy dose-rate distributions, there is a practical energy limit for simplification to a photon-only transport technique at the exclusion of coupled photon-electron transport, and high-energy photon-emitting radionuclides such as ¹⁹²Ir and ¹³⁷Cs may not be simulated accurately when close to the source. Electron contributions to the dosimetric uncertainty could be negligible given accurate transport equations, empirically derived atomic form factors, and proper implementation of the code by the dosimetry investigator. However, dosimetric differences within 1 mm of a ¹⁹²Ir source capsule between photon-only and coupled photon-electron transport may exceed 15%.^{49,50,57} Estimates of $k=1$ dosimetric uncertainties due to the physics

implementation within MC radiation transport algorithms at $r=1$ cm are 0.3% and 0.2% for low- and high-energy sources, respectively, and 0.7% and 0.3% at $r=5$ cm.^{43,47}

IV.G. Interaction and scoring cross sections

With the computational geometry established, progression of radiation transport is governed by atomic and nuclear cross sections that dictate the type and frequency of radiological interactions. These cross sections are organized into libraries that are maintained by international agencies such as the NNDC. Uncertainties in the cross sections within the source affect radiation emitted in the phantom. These cross sections are typically calculated and compared to experimental cross sections, determined at discrete energies. Given the physics model used to characterize the element and radiological interaction, a fitting function (such as a log-log fit) is used by the radiation transport code to interpolate between reported cross-section values. Since the interpolation fit may not be robust for all element and energy possibilities, it is recommended to use the recently derived cross-section libraries with high resolution in energy. Sensitivity of dosimetric results on cross-section libraries was illustrated by DeMarco *et al.*⁵⁸

MC-based radiation transport codes utilize μ_{en}/ρ toward calculating dose rates and are separated from μ/ρ as, for example, one could determine dose to muscle in water instead of dose to water in water. Here, the μ/ρ and μ_{en}/ρ values for water and muscle would be used, respectively. Thus, the uncertainties ($k=1$) in both μ/ρ and μ_{en}/ρ are of concern and are about 1.2% and 1.0% for low- and high-energy sources, respectively.^{59,60} The influence of the cross-section uncertainties on the absorbed dose is a function of distance from the source with larger distances subject to larger dosimetric uncertainties. For low-energy sources, the dosimetric uncertainties at 0.5 and 5 cm are about 0.08% and 0.76%, respectively; with high-energy sources, dosimetric uncertainties are 0.01% and 0.12% for these same distances.^{43,47} Further research on a modern assessment of cross-section uncertainties is needed.

IV.H. Scoring algorithms and uncertainties

All the prior steps set the simulation framework in which the calculations are performed. The dosimetry investigator must select the scoring algorithm used to determine the dose-rate distributions. While some estimators are more appropriate than others,⁶¹ none will truly represent the desired output resultant from the dosimetry calculations. Typically, some form of volume averaging or energy-weighted modification will be used to determine the dose rate at a given location within the calculation phantom. These uncertainties should be $<0.1\%$ for all classes (HDR/LDR and low/high energy) of brachytherapy sources. For path-length estimators used to determine collisional kerma, decreases in voxel thickness along the radial direction will diminish volume averaging within the voxel without significant influence on the type A uncertainties.⁶² However, MC estimators based on energy deposition within the voxel will have type A uncertainties

inversely proportional to the square root of the voxel volume and are thus influenced by voxel thickness along the radial direction. Derivation of brachytherapy dosimetry parameters such as Λ , $g(r)$, $F(r, \theta)$, and $\phi_{\text{an}}(r)$ using MC methods involves the summation of results over various tallied voxels, weighting results based on solid angle, or taking ratios of simulated dose rates. Since all brachytherapy dosimetry parameters are ratios of dose rates, except for Λ , it is often straightforward to simply take ratios of the raw simulated results. Systematic uncertainties in postsimulation processing may arise when energy thresholds δ ,² intentional volume averaging, or tally energy modifiers are employed. Further research on these uncertainties is needed.

V. UNCERTAINTY IN THE TG-43 DOSIMETRY FORMALISM PARAMETERS

What follows is a quantitative assessment of dosimetric uncertainties in the brachytherapy dosimetry parameters used in the TG-43 dose calculation formalism. The reader is directed to the 2004 AAPM TG-43U1 report for definitions of the brachytherapy dosimetry parameters.² The tables in the current report present best practice values for propagated uncertainties and are not meant to be used for uncertainty budgets.

V.A. Air-kerma strength

V.A.1. Uncertainty in NIST primary standard for LDR low-energy photon-emitting sources

The U.S. national primary standard of air-kerma strength ($S_{K,\text{NIST}}$) for low-energy (≤ 50 keV) photon-emitting brachytherapy sources, containing the radionuclide ^{103}Pd , ^{125}I , or ^{131}Cs , is realized using the NIST wide-angle free-air chamber (WAFAC).⁶³ The WAFAC is an automated, free-air ionization chamber with a variable volume. As of October 2010, over 1000 sources of 41 different designs from 19 manufacturers have been calibrated using the WAFAC since 1999. The expanded uncertainty ($k=2$) in $S_{K,\text{NIST}}$ is given as

$$V_{\text{WAFAC}} = 2\sqrt{(s_i^2 + u_j^2)}, \quad (1)$$

where s_i is equal to the standard deviation of the mean of replicate measurements (type A) and the quadrature sum of all type B components of uncertainty is represented by u_j (less than 0.8%).⁶⁴

Following the $S_{K,\text{NIST}}$ measurement, the responses of several well-type ionization chambers of different designs are measured at NIST. To understand the relationship between well-chamber response I and WAFAC-measured $S_{K,\text{NIST}}$ for low-energy photon brachytherapy sources, emergent photon spectra are measured with a high-purity germanium spectrometer. The relative response of calibration instruments has been observed to depend on both emergent spectrum and anisotropy.⁶⁴ Knowledge of source spectrum allows separation of well-chamber response effects due to spectrum differences from those caused by variations in the spatial anisotropy of emissions due to self-absorption by internal source components.

To verify that sources of a given design calibrated at NIST are representative of the majority of those calibrated in the past, several additional tests have been implemented. The distribution of radioactive material within a source is mapped using radiochromic film contact exposures. The in-air anisotropy of sources is studied by taking WAFAC and x-ray spectrometry measurements at discrete rotation angles about the long axis and the axis perpendicular to the mid-point of the source long axis, respectively. The “air-anisotropy ratio,” calculated from the results of angular x-ray measurements, has proven to be a useful parameter for explaining differences in well-chamber response observed for different source models having the same emergent spectrum on their transverse plane.⁶⁵ The first primary standard device in Europe for calibration of low-energy photon sources was the large-volume extrapolation chamber built at the PTB where the procedures are, in principle, the same as at NIST.⁶⁶ For each seed type (not necessarily for each individual seed of same type), the spectral photon distribution to obtain the spectrum dependent correction factors for air attenuation, scattering, etc., is determined. Details are given in Ref. 66. Using a sensitive scintillation detector free-in-air at 1 m, both polar and azimuthal anisotropies are measured for each individual seed to be calibrated. The results of the anisotropy measurements are part of the calibration certificate. The NPL also provides air-kerma rate calibrations of ¹²⁵I sources using their secondary standard radionuclide calibrator, a well-type ionization chamber for which the calibration coefficient is traceable to the NIST primary air-kerma standard.⁶⁴

V.A.2. Uncertainty in NIST primary standard for LDR high-energy photon-emitting sources

The U.S. national primary standard of $S_{K,NIST}$ for LDR high-energy gamma-ray-emitting brachytherapy sources containing the radionuclide ¹⁹²Ir is realized using a spherical graphite-wall cavity chamber that is open to the atmosphere.⁶⁷ Since arrays of approximately 50 sources were required to perform the cavity chamber measurement due to low detector-sensitivity, the $S_{K,NIST}$ of individual sources is determined by using a spherical-Al re-entrant chamber working standard with a ²²⁶Ra source to verify the stability of the re-entrant chamber over time. The expanded uncertainty ($k=2$) in $S_{K,NIST}$ for LDR ¹⁹²Ir sources is 2%. Well-chamber response is not as sensitive to small changes in source construction due to manufacturing variability for high-energy photon emitters in comparison to low-energy sources.⁶⁸ Nevertheless, additional characterization measurements are performed on the sources following calibration, including well-chamber response, photon spectrometry, and radiochromic film contact exposure measurements. The results of these measurements are used to verify that no significant modifications to the LDR low-energy source design have been implemented by the manufacturer.

Similar to ¹⁹²Ir, the U.S. national primary standard of $S_{K,NIST}$ for LDR high-energy photon-emitting brachytherapy sources containing ¹³⁷Cs is also realized using a spherical graphite-wall cavity chamber that is open to the

atmosphere.⁶⁹ For routine calibrations, a spherical-Al cavity chamber with several ¹³⁷Cs working standard sources is used. The expanded uncertainty ($k=2$) in $S_{K,NIST}$ for LDR ¹³⁷Cs sources is 2%. As is the case with LDR ¹⁹²Ir sources, well-chamber response is relatively insensitive to small changes in source construction. Additional characterization measurements performed on the sources following calibration include well-chamber response and radiochromic film contact exposure measurements.⁷⁰

At NPL, air-kerma rate calibrations are performed for ¹⁹²Ir wires and pins using the secondary standard radionuclide calibrator, which is traceable to the NPL air-kerma primary standard. The expanded uncertainty ($k=2$) for an ¹⁹²Ir air-kerma rate measurement is stated to be 1.5%.⁶⁵

V.A.3. S_K uncertainty for HDR high-energy sources

NIST traceability for the measurement of air-kerma strength for HDR ¹⁹²Ir sources is based on the interpolation of air-kerma calibration coefficients of a secondary standard ionization chamber.⁷¹ The weighted average-energy of these sources is 397 keV and thus an interpolated value between the calibration points of ¹³⁷Cs and 250 kVp x rays is used. However, more rigorous methodologies for the ionization chamber ¹⁹²Ir air-kerma calibration coefficient have been suggested,^{72,73} with Eq. (2) from Eq. (1) of Ref. 72,

$$\frac{1}{N_{S_K}^{Ir-192}} = \frac{1}{2} \left(\frac{1}{N_K^{Cs-137}} + \frac{1}{N_K^{x\text{ ray}}} \right), \quad (2)$$

which results in agreement within 0.5%, falling within the 2.15% uncertainty ($k=2$). $N_{S_K}^{Ir-192}$ is the ionization chamber air-kerma calibration coefficient for ¹⁹²Ir (or as designated ¹³⁷Cs or x ray).

There are two techniques to measure S_K using an ionization chamber calibrated as above, the shadow shield method and the seven-distance technique. The seven-distance technique has been refined and the results for S_K from all HDR ¹⁹²Ir source manufacturers have been found to agree to within 0.5%.⁷⁴ Air-kerma strength is thus given as

$$S_K = \frac{N_{S_K}^{Ir-192}(M_d - M_s)(d + c)^2}{\Delta t}, \quad (3)$$

where $N_{S_K}^{Ir-192}$ is the air-kerma calibration coefficient for ¹⁹²Ir, M_d is the direct measurement including the primary beam scatter M_s , distance to the source center d , setup distance error c , and irradiation time Δt . The value of S_K is then transferred to a well-type ionization chamber.

HDR ¹⁹²Ir air-kerma standards are established at LNHB, PTB, and NPL.⁷⁵ An intercomparison of the University of Wisconsin Accredited Dosimetry Calibration Laboratory (ADCL) calibration standard with the LNHB calibration standard showed agreement for a specific HDR ¹⁹²Ir source within 0.3%.⁷⁶ Intercomparisons done between NPL and LNHB demonstrated agreement to within 0.3% to 0.5%.⁷⁷ When uncertainty analysis is performed for all other HDR ¹⁹²Ir source models and intercomparisons, the overall expanded uncertainty ($k=2$) for S_K is 2.15%.^{73,74} LNHB

TABLE I. Propagation of best practice uncertainties ($k=1$ unless stated otherwise) associated with the transfer of air-kerma strength from NIST through the ADCL to the clinic for LDR low-energy brachytherapy sources.

Row	Measurement description	Quantity (units)	Relative propagated uncertainty (%)
1	NIST WAFAC calibration	$S_{K,NIST}$ (U)	0.8
2	ADCL well ion chamber calibration	$S_{K,NIST}/I_{ADCL}$ (U/A)	0.9
3	ADCL calibration of source from manufacturer	$S_{K,ADCL}$ (U)	1.1
4	ADCL calibration of clinic well ion chamber	$S_{K,ADCL}/I_{CLINIC}$ (U/A)	1.2
5	Clinic measures source air-kerma strength	$S_{K,CLINIC}$ (U)	1.3
	Expanded uncertainty ($k=2$)	$S_{K,CLINIC}$ (U)	2.6

achieves a HDR ^{192}Ir calibration uncertainty ($k=2$) of 1.3% for well-type ionization chambers.⁷⁶ Given the assortment of HDR high-energy sources and a variety of calibration methods used at the various primary standards laboratories, the aforementioned calibration uncertainties are not necessarily indicative for other sources or other laboratories.

V.A.4. Transfer of NIST standard to the ADCLs

The AAPM ADCLs are responsible for transferring a traceable calibration coefficient to the clinics. Therefore, the ADCLs maintain secondary air-kerma strength standards using well-type ionization chambers, which are directly traceable to NIST to a great precision and add about 0.1% to the uncertainty budget. The AAPM Calibration Laboratory Accreditation subcommittee monitors this traceability. ADCLs establish their on-site secondary standard by measuring the response of a well chamber to a NIST-calibrated source. The ratio of air-kerma strength S_K to I yields a calibration coefficient for a given source type. The ADCLs use their calibrated well chamber and manufacturer-supplied sources to calibrate well chambers for clinics. Calibrations of electrometers and instruments monitoring atmospheric conditions are also necessary to complete the system. For low-energy sources, intercomparisons among ADCLs and proficiency tests with NIST ensure that each ADCL is accurate in its dissemination, and that the calibrations from different ADCLs are equivalent. Europe does not yet have the same scale of infrastructure for low-energy source calibrations as does the U.S.

For LDR low-energy photon-emitting brachytherapy sources, the NIST air-kerma strength standard for each new source model is initially transferred to all ADCLs that are accredited by the AAPM to perform brachytherapy source calibrations by sending a batch of three WAFAC-calibrated sources, in turn, to each ADCL. To ensure that the NIST-traceable standard at each ADCL remains consistent over time with the initial baseline values, subsequent batches of three sources of each model are calibrated by NIST and circulated among all ADCLs at least annually.⁷⁸ A NIST-traceable air-kerma strength standard for both high-energy gamma-ray-emitting brachytherapy sources (i.e., ^{192}Ir and ^{137}Cs) has been available from all ADCLs for many years. Supplementary measurements performed at NIST, including I , photon spectrometry, and anisotropy characterization, provide quality assurance (QA) checks for WAFAC measure-

ments as well as the ability to monitor possible modifications in LDR low-energy seed construction. Data from NIST, the ADCLs, and the source manufacturer for each seed model are plotted as a function of time such that the integrity of the measurement traceability chain is verified. This process provides assurance that any ADCL secondary standard has not changed since the initial transfer within the uncertainty level, serving as a monitor for consistency. Based on the data collected by NIST and the ADCLs over many years, it appears that the accuracy achievable in a secondary standard is not the same for all source models. Variations in emergent spectrum and spatial anisotropy of emissions influence well chamber to WAFAC response ratios, and how well such variations are minimized during source fabrication affects the magnitude of variability in well-chamber measurements for sources of supposedly identical construction.

V.A.5. Transfer of NIST standard from ADCLs to the clinic

The use of an ADCL-calibrated well-ionization chamber is the usual manner for clinics to measure the strength of their brachytherapy sources. Therefore, the uncertainty in the well-chamber calibration coefficient for the specific type of source used is the key component that creates the final uncertainty in the air-kerma strength measured at the clinic.

Following the primary standard measurement of air-kerma strength ($S_{K,NIST}$), the response (usually a measured current I) of a well-ionization chamber is determined. The S_K/I ratio yields a calibration coefficient for the well-ionization chamber for a given source type. Such calibration coefficients enable well-ionization chambers to be employed at clinics for calibration of source air-kerma strength. To model the traceability of measurements performed on brachytherapy sources from the primary standard measurement of air-kerma strength at NIST to the transfer of this standard to the ADCLs and source manufacturers to a final verification of source strength at a clinic prior to their use in treatment, uncertainties have been assigned (based on NIST measurement histories) to $S_{K,NIST}$ and I as $\%u_{c,WAFAC}=0.8\%$ ($k=1$) and $\%u_{c,I}=0.5\%$ ($k=1$). These values are propagated through the measurement traceability chain in two paths, the first of which is shown in Table I. Although this model is applied to measurements of a single low-energy

TABLE II. Propagation of best practice uncertainties ($k=1$ unless stated otherwise) associated with the transfer of the air-kerma strength standard from NIST to the manufacturer for LDR low-energy brachytherapy sources.

Row	Measurement description	Quantity (units)	Relative propagated uncertainty (%)
1	NIST WAFAC calibration	$S_{K,NIST}$ (U)	0.8
2	Manufacturer well ion chamber calibration	$S_{K,NIST}/I_M$ (U/A)	0.9
3	Manufacturer calibration of QA source	$S_{K,M}$ (U)	1.1
4	Manufacturer instrument calibration for assay	$S_{K,M}/I_M$ (U/A)	1.2
5	Manufacturer assays production sources	$S_{K,M}$ (U)	1.3
6	Manufacturer places sources in 2% or 7% bins	$S_{K,M \text{ bin}}$ (U)	1.4 or 2.4
	Expanded uncertainty ($k=2$)	$S_{K,M \text{ bin}}$ (U)	2.8 or 4.8

photon-emitting source, the same analysis may be applied to high-energy photon-emitting sources by using the appropriate u_c values.

In row 1 of Table I, the air-kerma strength $S_{K,NIST}$ of a source is measured, which is then sent to an ADCL. The response of an ADCL standard well-ionization chamber is measured, yielding a current I_{ADCL} . A calibration coefficient for the chamber $S_{K,NIST}/I_{ADCL}$ is then calculated (row 2). The ADCL receives a source from the manufacturer (row 3), and the air-kerma strength $S_{K,ADCL}$ is calculated based on the standard well-chamber current measurement and the calibration coefficient for the chamber. To transfer the source calibration to the clinic, a well chamber from the clinic is sent to an ADCL, where the calibration coefficient $S_{K,ADCL}/I_{CLINIC}$ is determined (row 4). Finally, in row 5, the well-chamber ionization current is measured and multiplied by the calibration coefficient, yielding an air-kerma strength $S_{K,CLINIC}$ for the clinical source. According to this model, the propagation of uncertainties from the various well-chamber measurements involved in the transfer of the source-strength standard to the clinic results in a minimum expanded uncertainty ($k=2$) in $S_{K,CLINIC}$ of 2.56%. This level of uncertainty assumes that the clinic is measuring a single seed with a high-quality electrometer and other reference-quality measurement equipment. An alternate method of calibration, instead of the well-chamber calibration, is for the clinic to purchase a source and send it to the ADCL for calibration. When this calibrated source is sent to the clinic, it is used to calibrate the clinic's well chamber. This procedure results in an additional uncertainty of 0.6%, resulting in a total uncertainty of 2.83% at $k=2$.

The second path of the measurement traceability chain is illustrated in Table II. Following measurement of air-kerma strength $S_{K,NIST}$ at NIST, a source is returned to the manufacturer. The response of a manufacturer's well-ionization chamber is measured, yielding a current I_M . A calibration coefficient for the chamber $S_{K,NIST}/I_M$ is then calculated (row 2). For QA purposes, the air-kerma strength $S_{K,M}$ of a reference source is calculated based on well-chamber current measurements and the chamber calibration coefficient (row 3). This reference source is used to determine the calibration coefficient $S_{K,M}/I_M$ for a well-ionization chamber located on the source production line (row 4). To verify source strength as part of the production process, the well-chamber ioniza-

tion current is measured and multiplied by the calibration coefficient, yielding an air-kerma strength $S_{K,M}$ for the source (row 5). Finally, in row 6, the source is placed in a 2% wide bin with other sources of air-kerma strength $S_{K,M \text{ bin}} \pm 1\%$. Some manufacturers have larger bin sizes, up to 7% wide. Therefore, a range is included in row 6 of Table II to account for the range in bin sizes. The source is then sent to a clinic for patient treatment. According to this model, the propagation of uncertainties from the various well-chamber measurements involved in the transfer of the source-strength standard to the manufacturer, including binning, results in a minimum expanded uncertainty ($k=2$) in $S_{K,M \text{ bin}}$ of 2.83%. To evaluate the uncertainty due to binning, the binning process is treated as an additive perturbation such that

$$S_{K,M \text{ bin}} = S_{K,M} + B, \quad (4)$$

where B is the bias associated with placing a seed of air-kerma strength $S_{K,M}$ in a bin of center value $S_{K,M \text{ bin}}$. The bin width is modeled by a rectangular distribution, yielding a component of uncertainty due to binning of 0.6% for a 2% wide bin and 2.0% for a 7% wide bin. The minimum uncertainty in $S_{K,M \text{ bin}}$ ($k=2$) is therefore 2.81%, increasing to 4.78% for the widest bin in this model (row 6 in Table II).

Now the question may be asked, "How well should the clinical determination of source air-kerma strength ($S_{K,CLINIC}$) based on an ionization current measurement in a calibrated well chamber agree with the value ($S_{K,M \text{ bin}}$) provided by the manufacturer?" To answer this question, one must first establish a source acceptance criterion. One possibility is to require that the absolute value of the difference between the air-kerma strength stated by the manufacturer $S_{K,M \text{ bin}}$ and that determined by the clinic $S_{K,CLINIC}$ be less than the propagated uncertainty of that difference with an appropriate coverage factor according to

$$|S_{K,CLINIC} - S_{K,M \text{ bin}}| < \sqrt{V_{S_{K,CLINIC}}^2 + V_{S_{K,M \text{ bin}}}^2 - V_{S_{K,WAFAC}}^2}. \quad (5)$$

Since $V_{S_{K,WAFAC}}$ is common to both paths of the measurement traceability chain, it is removed (in quadrature) so as not to be added twice. Using the uncertainties determined from the model at the ends of the two paths of the measurement traceability chain, $S_{K,CLINIC}$ must agree with $S_{K,M \text{ bin}}$ to within 3.4% (assuming 2% bins) in order for the source to be

TABLE III. Propagation of best practice uncertainties ($k=1$ unless stated otherwise) associated with the transfer of air-kerma strength from NIST through the ADCL to the clinic for LDR high-energy brachytherapy sources. Well-chamber measurement uncertainty is estimated to be 0.5 %.

Row	Measurement description	Quantity (units)	Relative propagated uncertainty (%)
1	NIST calibration	$S_{K,NIST}$ (U)	1.0
2	ADCL well ion chamber calibration	$S_{K,NIST}/I_{ADCL}$ (U/A)	1.1
3	ADCL calibration of source from manufacturer	$S_{K,ADCL}$ (U)	1.2
4	ADCL calibration of clinic well ion chamber	$S_{K,ADCL}/I_{CLINIC}$ (U/A)	1.3
5	Clinic measures source air-kerma strength	$S_{K,CLINIC}$ (U)	1.4
	Expanded uncertainty ($k=2$)	$S_{K,CLINIC}$ (U)	2.8

acceptable for use by the clinic. This result is for a set of measurements made on a single source and does not include uncertainties due to source-to-source variability. Thus, 3.4% is the lower limit for the source acceptance criterion. Criterion for acceptance of calibration is discussed in Ref. 79, where the lower-third of its Table II for 100% source assay is directly comparable to Table II of the current report.

In the case of high-energy sources, the procedure is similar to that given above with some minor differences. For LDR high-energy sources, there are long-lived sources, such as ^{137}Cs , and shorter-lived sources, such as ^{192}Ir sources. Table III is presented for the clinic measurement uncertainty with an ADCL-calibrated well-ionization chamber and is certainly appropriate for a short-lived source. Following the same model of uncertainty propagation as above (assuming $\%u_{c,I}=0.5\%$ for each well-chamber measurement), the minimum expanded uncertainty ($k=2$) of clinical air-kerma strength measurements for LDR high-energy sources is 2.8% (Table III). In the case of a long-lived source, the original NIST-calibrated source may be used, in which case, rows 2 and 3 are not present. In this case, the uncertainty in the ADCL calibration of the clinic well chamber is 1.12% and the uncertainty in the clinical measurement is 1.22%, with the expanded uncertainty of 2.45% ($k=2$). The HDR high-energy sources have a NIST-traceable calibration through an interpolated calibration coefficient from two photon beams as given in Ref. 71. Following the same model of uncertainty propagation as above (assuming 0.5% uncertainty on each well-chamber measurement), the minimum expanded uncertainty ($k=2$) of clinical S_K measurements for HDR high-energy sources is 2.94% from Table IV.

TABLE IV. Propagation of best practice uncertainties ($k=1$ unless stated otherwise) associated with the transfer of air-kerma strength from a traceable NIST coefficient from the ADCL to the clinic for HDR high-energy brachytherapy sources.

Row	Measurement description	Quantity (units)	Relative propagated uncertainty (%)
1	ADCL calibration	$S_{K,NIST}$ (U)	1.1
2	ADCL well ion chamber calibration	$S_{K,NIST}/I_{ADCL}$ (U/A)	1.2
3	ADCL calibration of source from manufacturer	$S_{K,ADCL}$ (U)	1.3
4	ADCL calibration of clinic well ion chamber	$S_{K,ADCL}/I_{CLINIC}$ (U/A)	1.4
5	Clinic measures source air-kerma strength	$S_{K,CLINIC}$ (U)	1.5
	Expanded uncertainty ($k=2$)	$S_{K,CLINIC}$ (U)	2.9

V.B. Dose-rate constant

As Λ is defined as the ratio of dose rate at the reference position to the air-kerma strength, $\Lambda \equiv \dot{D}(r_0, \theta_0)/S_K$, the Λ uncertainty is simply

$$\%u_{\Lambda} = \sqrt{\%u_{\dot{D}(r_0, \theta_0)}^2 + \%u_{S_K}^2}. \quad (6)$$

While Sec. V A 5 discussed $u_{S_{K,CLINIC}}$, clinical users do not measure the reference dose rate and thus do not directly obtain $\%u_{\Lambda}$. Instead, $\%u_{\Lambda}$ values are taken from the literature of dosimetry investigators upon deriving Λ . For instance, when the AAPM issues consensus datasets, Λ and $\%u_{\Lambda}$ consensus values may be provided with $\%u_{\Lambda}$ values generally smaller than the individual investigator $\%u_{\Lambda}$ value due to increased sampling of candidate datasets. For low- and high-energy photon-emitting brachytherapy sources, the measured values of $\%u_{\Lambda}$ ($k=1$) are approximately 2.9%; MC-simulated values of $\%u_{\Lambda}$ ($k=1$) are approximately 2.1%.

V.C. Geometry function

The geometry function is dependent on L (or effective length), r , and θ . Since L is primarily used to minimize interpolation errors during treatment planning, it can take on almost any value.^{62,80,81} However, realistic dose distributions are usually best-approximated through using realistic L values. In practice, the geometry function is used by dosimetry investigators to determine other parameters such as $g(r)$ and $F(r, \theta)$. In both cases, the geometry function is used to remove the effects of solid angle when evaluating measurements or calculations of dose rate around a source. Conse-

quently, the geometry function appears in both the numerator and the denominator of the expressions used to determine these parameters. A proper uncertainty analysis will recognize the artificial decoupling of the TG-43 brachytherapy dosimetry parameters, and that the geometry function cancels out once dose-rate values are obtained in the TPS as long as it is used consistently in the other parameters such as $g(r)$ and $F(r, \theta)$. Variability in dose measurements resulting from the associated variability in source positioning contributes to dosimetric uncertainties, not geometry function uncertainties. Thus, the practical implementation of the geometry function means there is no associated uncertainty. That is, $\%u_{G(r, \theta)} = 0$. While sources of a given model have L variations, these variations manifest themselves with physical dose rates and other parameters because a single consistent L is used for a given source model.⁸¹

V.D. Radial dose function

The radial dose function uncertainty is the square root of the sum of the squares of the relative dose-rate uncertainties at the reference position and point of interest on the transverse plane. In Sec. V C, it was shown that the geometry function uncertainty was zero. Thus,

$$\%u_{g(r)} = \sqrt{\%u_{\dot{D}(r_0, \theta_0)}^2 + \%u_{\dot{D}(r, \theta_0)}^2}. \quad (7)$$

In general, the uncertainty increases for large r (more for low-energy sources where attenuation is greater) and for small r (based on dosimetric uncertainties close to the source). Estimates of this type B uncertainty are based on the experience gained through the derivation of a large number of AAPM consensus datasets from candidate datasets.² For $0.5 \text{ cm} \leq r \leq 5 \text{ cm}$, low- and high-energy photon-emitting brachytherapy source measured values of $\%u_{g(r)}$ ($k=1$) are approximately 2% and 1%, respectively; MC-simulated values of $\%u_{g(r)}$ ($k=1$) are approximately 1% and 0.5%, respectively. These dose uncertainties increase for $r < 0.5 \text{ cm}$ due to the influence of dynamic internal components and for $r > 5 \text{ cm}$ due to cross-section uncertainties in the phantom material.

V.E. 2D anisotropy function

The 2D anisotropy function uncertainty is the square root of the sum of the squares of the relative dose-rate and geometry function uncertainties. It was shown that the geometry function uncertainty was zero in Sec. V C. Thus,

$$\%u_{F(r, \theta)} = \sqrt{\%u_{\dot{D}(r, \theta)}^2 + \%u_{\dot{D}(r, \theta_0)}^2}. \quad (8)$$

In general, the uncertainty increases with increasing r and when θ approaches the long axis of the source due to diminished dose rates. As θ approaches 90° , $\%u_{F(r, \theta)}$ approaches zero. The numerator and denominator of $F(r, \theta)$ share the same r , and uncertainties due to cross section or medium corrections are minimized. Estimates of this type B uncertainty are based on the experience gained through the derivation of a large number of AAPM consensus datasets from

candidate datasets.² For low- and high-energy sources, measured $\%u_{F(r, \theta)}$ ($k=1$) uncertainties are approximately 2.4% and 1.3%, respectively; MC-simulated values of $\%u_{F(r, \theta)}$ ($k=1$) are approximately 1.1% and 0.6%, respectively. These uncertainties are weighted over all polar angles and are substantially larger near the source long axis where dynamic internal components may cause large dose variations.

V.F. 1D anisotropy function

Since the 1D anisotropy function is the average of the dose rate around the source at a given r divided by the dose rate on the transverse plane at the same r , it is a relative function just like $g(r)$ and $F(r, \theta)$. Because of the volume averaging, it is more complicated to express the dosimetric uncertainty at a given radius since the $4\pi \text{ sr}$ averaging may require exclusion of the capsule. However, its expression is similar to that for the 2D anisotropy function,

$$\%u_{\phi_{\text{an}}(r)} = \sqrt{\%u_{\int \dot{D}(r, \theta) d\theta}^2 + \%u_{\dot{D}(r, \theta_0)}^2}. \quad (9)$$

In practice, $\%u_{\phi_{\text{an}}(r)}$ is less than $\%u_{F(r, \theta)}$ due to diminishment of positioning uncertainties due to volume/angular averaging. As for $g(r)$ and $F(r, \theta)$, uncertainties increase for large r (diminishment of dose rate) and for small r based on dosimetric uncertainties close to the source. Estimates are based on the determination of $F(r, \theta)$ uncertainty (Sec. V E). For low- and high-energy sources, measured $\%u_{\phi_{\text{an}}(r)}$ ($k=1$) uncertainties are approximately 1.5% and 1.1%, respectively; MC-simulated values of $\%u_{\phi_{\text{an}}(r)}$ ($k=1$) are approximately 0.6% and 0.4%, respectively.

V.G. TPS uncertainties summary

The uncertainty in TPS-calculated dose will be based on the combination of uncertainties of NIST-traceable S_K and the dose rates determined by the dosimetry investigator. However, there are additional uncertainties introduced by the TPS.

Commissioning of the brachytherapy source for dose calculations requires the physicist or other responsible person to install source characterization data into the TPS computer. Since primary calculations for patient treatment are almost never performed today using manual methods, other than for a check, the uncertainty associated with manual calculations will not be discussed. Therefore, the question becomes, what additional uncertainty is associated with the installation of source characterization data, and the use of those data in the TPS, to calculate dose distributions?

When dosimetry parameters are entered, the frequency and spacing of the data are key since the TPS performs interpolation on the entered data. Unless spacing varies in inverse proportion to the contribution of a parameter, the uncertainty is likely to be different at different distances. When fits to experimental- or MC-derived dosimetry parameters are entered, the uncertainty relates to the quality of the fit. The fit approach and model used will affect the uncertainty. Further, the TPS dose calculation uncertainty depends on the implementation of the algorithm, the calculation matrix spac-

TABLE V. Propagation of best practice uncertainties ($k=1$ unless stated otherwise) in dose at 1 cm on the transverse plane associated with source-strength measurements at the clinic, brachytherapy dose measurements or simulation estimates, and treatment planning system dataset interpolation for low-energy (*low-E*) and high-energy (*high-E*) brachytherapy sources as relating to values presented in Fig. 1.

Row	Uncertainty component	Relative propagated uncertainty (%)	
		<i>low-E</i>	<i>high-E</i>
1	S_K measurements from row 5 of Tables I and IV	1.3	1.5
2	Measured dose	3.6	3.0
3	Monte Carlo dose estimate	1.7	1.6
4	TPS interpolation uncertainties	3.8	2.6
5	Total dose calculation uncertainty	4.4	3.4
	Expanded uncertainty ($k=2$)	8.7	6.8

ing, and the veracity of the output mechanisms. Consequently, it is impossible to determine explicitly the uncertainty introduced by model fitting and interpolation. Based on the experience gained through the derivation of a large number of AAPM consensus datasets from candidate datasets,² $\%u_{\text{TPS}}$ values ($k=1$, type B) of 3.8% and 2.6% are recommended for low- and high-energy sources, respectively, unless specific data indicate otherwise. These values are slightly higher than the 2% ($k=1$) value in the 2004 TG-43U1 report which pertained to individual dosimetry parameters.

Propagating the uncertainties from all components (see Sec. V and Table V) to obtain the dose at 1 cm on the brachytherapy source transverse plane, the $k=2$ uncertainties for low- and high-energy sources are $\%V_D=8.7\%$ and $\%V_D=6.8\%$, respectively. Note that these uncertainty estimates are generalized for the broad variety of available sources in each source photon energy classification and are restricted to single-source dose distributions in a standardized liquid water spherical phantom.

VI. RECOMMENDATIONS

Uncertainty analyses should include all dosimetric properties of clinical brachytherapy sources and follow a common set of guidelines and principles, analogous to TG-43 parameters for brachytherapy sources. We recommend following the principles described in Secs. I and II of the current report. This will provide more accurate and meaningful determination of dose in treatment plans and facilitate comparison between multiple investigators. The goal is to quantify overall uncertainty in the delivered dose and maintain it at the lowest possible level.

VI.A. General uncertainty

Uncertainty analyses should be performed using a universal methodology. The recommended methodology (i.e., GUM) was described in detail in Sec. II of the current report and is fully documented in NIST Technical Note 1297.¹⁰ AAPM/GEC-ESTRO recommends that when reporting uncertainties of physical quantities relevant to brachytherapy (e.g., air-kerma strength, absorbed dose, and dose rate), the

expanded uncertainty should be given along with the measured value of the quantity using a coverage factor of 2 ($k=2$). Moreover, the current report has adopted the symbol V to indicate expanded uncertainty to avoid confusion with the symbol U , which is commonly used by the medical physics community to indicate S_K units. In addition, all components of uncertainty, identified as type A or type B, should be tabulated along with the calculated value of the combined standard uncertainty. The statistical methods used to obtain the various components of u_c should be described in detail, and a *level of confidence* interpretation of the results may be included, if appropriate.

VI.B. Clinical medical physicists

VI.B.1. S_K and TPS data entry

To minimize uncertainties, clinical medical physicists should use the consensus brachytherapy dosimetry data. The use of nonconsensus data would lead to a mistake (see Sec. II) rather than an increase in uncertainties. The primary aspects under control by the clinical medical physicist are measurements of S_K and TPS data entry. For the first aspect, the clinical medical physicist should follow the 2008 AAPM brachytherapy source calibration recommendations.⁷⁹ For TPS data entry, the physicist should carefully consider the recommendations of Sec. V G and avoid inadvertently increasing the uncertainties by, for example, deviating from the numerical or spatial resolution of the AAPM-recommended consensus dataset.² Here, the 2% tolerances associated with dataset interpolation may increase with a coarser dataset. Another example of a local uncertainty exceeding the best practice values in the current report would be the use of a novel source with a calibration certificate indicating higher S_K uncertainties than presented in Sec. V A.

VI.B.2. Treatment planning system developments

It is important for the clinical medical physicist to keep an eye toward the future regarding efforts to improve the current TG-43 dose calculation formalism. These improvements might include development of dose calculation algorithms to account for intersource attenuation, phantom scatter, and material heterogeneities.⁷ Currently, there is an infrastructure in

place for dosimetry investigators, source manufacturers, TPS manufacturers, clinical medical physicists, and professional societies to promote consistent usage of a standardized dataset (i.e., TG-43 dosimetry parameters) for a single-source model. As dose calculation algorithms become more sophisticated, these standardized datasets will no longer be directly used for derivation of patient dose.⁸² Consequently, the clinical medical physicist must note the changes in dose calculation uncertainty as TPS manufacturers migrate toward more sophisticated algorithms. This topic is under investigation by AAPM TG-186.

VI.B.3. Clinical dosimetric uncertainties

While lower uncertainties are clearly better, what maximum uncertainty should be clinically acceptable? Like the joint ABS/ACMP/ACRO report,⁸³ the AAPM and GEC-ESTRO also recommend actions be taken to reduce the uncertainty in dose delivery for a particular patient implant such as applicator repositioning, written directive adjustment, or procedure termination. However, the AAPM and GEC-ESTRO recognize that at this time the clinical medical physicist is unlikely to be able to accurately determine the dosimetric uncertainties in multiple sources because no specific recommendations have been published. Clinical practice recommendations on the uncertainty of the dose deviation have not been previously provided. Table V summarizes dosimetric uncertainty contributions that lead to an overall expanded uncertainty of less than 10% ($k=2$) for conventional photon-emitting brachytherapy sources. Yet there may be sources in which these dosimetric uncertainties are larger, such as when using investigational sources that lack a robust source-strength calibration traceable to a primary standards laboratory, or for sources whose calibration carries uncertainties larger than those in row 1 of Table V due to design variations and subsequent energy differences.⁸⁴ These circumstances and other factors may result in increased dosimetric uncertainties as recognized previously by Nag *et al.*⁸³ When these uncertainties add to those for sources of Table V and exceed 20% ($k=2$), then the AAPM and GEC-ESTRO recommend that brachytherapy implants be performed with caution—preferably under Institutional Review Board (IRB) oversight with prior disclosure to the patient about the uncertain aspects of the procedure.

VI.C. Dosimetry investigators

When performing physical measurements, investigators are encouraged to identify as many sources of uncertainty as possible. Several potential sources of uncertainty in physical measurements performed on brachytherapy sources exist. Many of these have been presented in Sec. III. Other sources of uncertainty may exist and, therefore, it is up to the individual investigators to determine other potential uncertainties and evaluate them appropriately. However, the specific areas of uncertainty presented in the current report should be addressed in articles providing dosimetry parameters for brachytherapy sources and should include:

- (i) Positional uncertainty: When evaluating measurement position uncertainty, both source and detector positional uncertainty should be evaluated. In addition to source-to-detector distance uncertainty, angular uncertainty and its effect on the measured quantity should be addressed. Tolerances for specific source positioning jigs and phantom construction should be included in the uncertainty analysis. Moreover, due to the nature of the radiation emitted from brachytherapy sources, the magnitude of the uncertainty often depends on the distance from the source, as described in Sec. III A 2. Efforts should be made to address this behavior.
- (ii) Dose measurement: Brachytherapy source dosimetry investigations usually involve the quantification of dose from the source. When performing such measurements, the investigator must account for specific detector characteristics for the energy being measured and their role in overall uncertainty. The lowest possible uncertainty that is achievable will come from choosing the best instrument for the experimental investigation. Therefore, dosimeters should be chosen with care. The reported uncertainty should reflect the authors' understanding of the various available dosimeters. For example, an investigation using TLDs should specify the annealing regime used as this can result in an increase in the uncertainty from 1% to 5%, depending on the temperature and the cooling rate procedure.¹⁹ In addition, uncertainties arise from the differences in TLD response due to differing photon energy of the calibration source (e.g., 1.25 MeV) and low-energy brachytherapy sources (e.g., 0.03 MeV). This energy dependence may be divided into intrinsic energy dependence $k_{Bq}(Q)$ (relating detector reading to detector dose) and absorbed-dose energy dependence $f(Q)$ (relating dose to a detector to dose to medium in the absence of the detector).¹⁸ When measuring the absorbed dose for low-energy photon-emitting brachytherapy sources when calibrating with a ⁶⁰Co beam, the $k_{Bq}(Q)$ uncertainty ($k=1$) can be significantly less than 5%.^{2,18}
- (iii) Measurement medium: The AAPM TG-43 brachytherapy dosimetry protocol specifies a methodology to determine the absorbed dose to water for a brachytherapy source. The difficulties involved with measurements in a liquid medium often result in experiments being carried out in a solid medium that is designed to be radiologically equivalent to liquid water. However, many of the materials on the market today have been designed to be water equivalent at a particular energy range, usually megavoltage photon energies. These materials may or may not be equivalent to water at lower photon energies or for other types of radiation. Investigators should address the impact that measurement medium will have on the results as it pertains to absorbed dose to water. In addition, measurement phantom size should be specified in the investigators' publications.

As with physical measurements, MC simulations also contain uncertainties in their results. As such, MC investigators should have a thorough understanding of the MC process and its associated uncertainties. Specific areas to be addressed are as follows:

- (i) Type A uncertainties: MC methods are stochastic in nature. By using probability distributions, appropriate starting conditions, and suitable pseudorandom numbers, a problem may be simulated to produce a result consistent with a physical system. In general, convergence of MC-based radiation transport simulations obey Poisson statistics and, as such, have an associated statistical uncertainty that decreases as the inverse square root of the number of samples (in this case the number of particle histories). Thus, the investigator should provide simulations with a sufficient number of histories to provide an acceptable level of statistical uncertainty ($<0.1\%$) so these may be considered negligible in comparison to other less constrainable uncertainties.
- (ii) Type B uncertainties: In addition to the type A uncertainties that arise naturally from a MC simulation, any model of a physical system will include type B uncertainties. This type of uncertainty will consist of uncertainties in source dimensions, internal component location(s), volume averaging, and material composition, for example. A thorough investigation to determine as many of the type B uncertainties as possible and their effects on the dosimetric quantities should be performed in the course of completing a MC study of a brachytherapy source. Examples of determining the type B uncertainties for a brachytherapy source have been given throughout Secs. III and IV.

VI.D. Source and TPS manufacturers

Brachytherapy source manufacturers should implement tight tolerances on their manufacturing processes since the clinical results are dependent on consistent source fabrication. The largest potential dosimetric variation is from dynamic internal components (Sec. IV B). Thus, the design should constrain motion of these components. The source design/version in regular clinical use should be the same design/version measured and simulated by the dosimetry investigator and measured by the dosimetry laboratories. Moreover, detailed information on the source components including dimensions, tolerances, and material compositions should be openly provided. If the manufacturer decides to change source design/version, the manufacturer must recognize that this is equivalent to construction of a new source, which is subject to the processes described by DeWerd *et al.*,⁷⁸ which include regular comparisons with dosimetry laboratories. Furthermore, manufacturers are advised to minimize and keep constant any radiocontaminants per Sec. IV C.

As mentioned in Sec. VI C, it is recommended that TPS manufacturers continue to strive for clinical utilization of

standardized datasets and development of TPS algorithm benchmarking procedures toward minimizing type B dose calculation uncertainties. This can be accomplished through continuing adoption of the consensus dataset approach for single-source dose calculations in standardized geometries and through providing the information required to dosimetrically characterize the clinical applicators and patient interfaces which will be incorporated in these new TPS platforms.

VII. SUMMARY AND COMPARISON TO EXISTING WRITTEN STANDARDS

Throughout the current report, the AAPM and GEC-ESTRO have refined clinical expectations of brachytherapy dosimetric uncertainty. Uncertainties are involved in all aspects of the dosimetry process. Every aspect of the process results in a greater uncertainty in the estimation of patient dose. The AAPM TG-40 and TG-56 reports attempted to provide QA procedures to reduce dosimetric uncertainty.^{1,70} The end result for consideration is the uncertainties involved in patient treatments. The first aspect of these uncertainties involves the transfer of the NIST calibration standard from the ADCL to the clinic's well chamber for the determination of measured source strength. When the clinical medical physicist measures this, a typical uncertainty ($k=2$) is about 3% (Sec. V A 5). If each source is not measured, the corresponding uncertainty is increased through use of the manufacturer value based on batch averaging. If the physicist relies solely on the manufacturer's value, then unknown manufacturer measurement uncertainties are passed along to the clinic (patient), along with possible administrative errors by the manufacturer sending sources from the order placed by another institution. Generally, the manufacturer source-strength uncertainty is larger than if measured by the clinical medical physicist using an instrument with a calibration coefficient traceable to a primary standards laboratory.⁷⁹ The second aspect of dosimetric uncertainty involves treatment planning. Intrinsic to this process is derivation and utilization of TG-43 parameters. If these parameters are based on AAPM consensus data, their uncertainties should have been provided in the AAPM report. If data from multiple dosimetry investigators are entered into the TPS, the resultant dosimetric uncertainty of the calculated dose is greater. Further, uncertainties in the treatment planning process are not as great an effect on the patient treatment as is the initial determination of the reference dose-rate distribution. When all these uncertainties are combined, the $k=2$ uncertainty of dose rates for low- and high-energy photon-emitting brachytherapy sources used in treatment planning are approximately 9% and 7%, respectively. Uncertainty in dose delivery due to physical implantation will add to these uncertainties and surely be larger upon clinical implementation. Consequently, it is paramount that the clinical medical physicist be cognizant of these uncertainties and endeavor to minimize them for the aspects within their responsibilities. Similarly, brachytherapy source dosimetry investigators should continue to minimize dosimetric uncertainties in their reference data.

The AAPM TG-56 report recommends brachytherapy dose delivery accuracy within 5%–10% with source calibration accuracy within 3%.⁷⁰ This latter tolerance was updated by Butler *et al.*⁷⁹ to 6% for individual sources. While the scope of the current report is limited to evaluation of pre-treatment brachytherapy dosimetry uncertainties, it appears that the TG-56 10% criterion for accuracy of brachytherapy dose delivery cannot be adhered to within a 95% confidence level. To our knowledge, there are no other existing societal standards on uncertainty for brachytherapy source calibration and dose delivery, and additional research in this area is needed. A joint effort of GEC-ESTRO and AAPM brachytherapy physicists/physicians will explore more details of the clinical aspects of the total uncertainty budget for brachytherapy treatment delivery.

ACKNOWLEDGMENTS

The authors extend their appreciation to the AAPM, GEC-ESTRO, and *Medical Physics* reviewers who helped to improve this report while considering the practical aspects for clinical implementation.

^{a)}Electronic mail: mrivard@tuftsmedicalcenter.org

- ¹G. J. Kutcher, L. Coia, M. Gillin, W. F. Hanson, S. Leibel, R. J. Morton, J. R. Palta, J. A. Purdy, L. E. Reinstein, G. K. Svensson, M. Weller, and L. Wingfield, "Comprehensive QA for radiation oncology: Report of AAPM Radiation Therapy Committee Task Group No. 40," *Med. Phys.* **21**, 581–618 (1994).
- ²M. J. Rivard, B. M. Coursey, L. A. DeWerd, W. F. Hanson, M. S. Huq, G. S. Ibbott, M. G. Mitch, R. Nath, and J. F. Williamson, "Update of AAPM Task Group No. 43 Report: A revised AAPM protocol for brachytherapy dose calculations," *Med. Phys.* **31**, 633–674 (2004).
- ³R. Nath, L. L. Anderson, G. Luxton, K. A. Weaver, J. F. Williamson, and A. S. Meigooni, "Dosimetry of interstitial brachytherapy sources: Recommendations of the AAPM Radiation Therapy Committee Task Group No. 43," *Med. Phys.* **22**, 209–234 (1995).
- ⁴M. J. Rivard, W. M. Butler, L. A. DeWerd, M. S. Huq, G. S. Ibbott, A. S. Meigooni, C. S. Melhus, M. G. Mitch, R. Nath, and J. F. Williamson, "Supplement to the 2004 update of the AAPM Task Group No. 43 Report," *Med. Phys.* **34**, 2187–2205 (2007).
- ⁵J. D. Honsa and D. A. McIntyre, "ISO 17025: Practical benefits of implementing a quality system," *J. AOAC Int.* **86**, 1038–1044 (2003).
- ⁶J. A. C. Sterne and G. D. Smith, "Sifting the evidence—What's wrong with significance tests?," *BMJ* **322**, 226–231 (2001).
- ⁷M. J. Rivard, J. L. M. Venselaar, and L. Beaulieu, "The evolution of brachytherapy treatment planning," *Med. Phys.* **36**, 2136–2153 (2009).
- ⁸P. Giacomo, "News from the BIPM," *Metrologia* **17**, 69–74 (1981).
- ⁹Evaluation of measurement data—Guide to the expression of uncertainty in measurement, *International Organization for Standardization (ISO)*, Joint Committee for Guides in Metrology (JCGM 100, 2008), corrected version 2010, http://www.bipm.org/utis/common/documents/jcgm/JCGM_100_2008_E.pdf (last accessed December 5, 2010).
- ¹⁰B. N. Taylor and C. E. Kuyatt, "Guidelines for evaluating and expressing the uncertainty of NIST measurement results," NIST Technical Note 1297 (U.S. Government Printing Office, Washington, DC, 1994), <http://physics.nist.gov/Pubs/guidelines/contents.html> (last accessed December 5, 2010).
- ¹¹M. J. Rivard, C. S. Melhus, and B. L. Kirk, "Brachytherapy dosimetry parameters calculated for a new ¹⁰³Pd source," *Med. Phys.* **31**, 2466–2470 (2004).
- ¹²M. J. Rivard, B. L. Kirk, and L. C. Leal, "Impact of radionuclide physical distribution on brachytherapy dosimetry parameters," *Nucl. Sci. Eng.* **149**, 101–106 (2005).
- ¹³M. G. Mitch and S. M. Seltzer, "Model-specific uncertainties in air-kerma strength measurements of low-energy photon-emitting brachytherapy sources," *Med. Phys.* **34**, 2337 (2007).
- ¹⁴R. C. Taylor, G. S. Ibbott, and N. Tolani, "Thermoluminescence dosimetry measurements of brachytherapy sources in liquid water," *Med. Phys.* **35**, 4063–4069 (2008).
- ¹⁵R. Taylor, G. Ibbott, S. Lampe, W. Bivens-Warren, and N. Tolani, "Dosimetric characterization of a ¹³¹Cs brachytherapy source by thermoluminescence dosimetry in liquid water," *Med. Phys.* **35**, 5861–5868 (2008).
- ¹⁶S. W. Peterson and B. Thomadsen, "Measurements of the dosimetric constants for a new ¹⁰³Pd brachytherapy source," *Brachytherapy* **1**, 110–119 (2002).
- ¹⁷T. Kron, L. DeWerd, P. Mobit, J. Muniz, A. Pradhan, M. Toivonen, and M. Waligorski, "A checklist for reporting of thermoluminescence dosimetry (TLD) measurements," *Phys. Med. Biol.* **44**, L15–L19 (1999).
- ¹⁸L. A. DeWerd, L. J. Bartol, and S. D. Davis, "Thermoluminescence dosimetry," in *Clinical Dosimetry for Radiotherapy: AAPM Summer School*, edited by D. W. O. Rogers and J. E. Cygler (Medical Physics Madison, WI, 2009), pp. 815–840.
- ¹⁹J. A. Raffi, S. D. Davis, C. G. Hammer, J. A. Micka, K. A. Kunugi, J. E. Musgrove, J. W. Winston, Jr., T. J. Ricci-Ott, and L. A. DeWerd, "Determination of exit skin dose for ¹⁹²Ir intracavitary accelerated partial breast irradiation with thermoluminescent dosimeters," *Med. Phys.* **37**, 2693–2702 (2010).
- ²⁰P. T. Muench, A. S. Meigooni, R. Nath, and W. L. McLaughlin, "Photon energy dependence of the sensitivity of radiochromic film compared with silver halide and LIF TLDs used for brachytherapy dosimetry," *Med. Phys.* **18**, 769–775 (1991).
- ²¹M. C. Saylor, T. T. Tamargo, W. L. McLaughlin, H. M. Khan, D. F. Lewis, and R. D. Schenfele, "A thin film recording medium for use in food irradiation," *Radiat. Phys. Chem.* **31**, 529–536 (1988).
- ²²S.-T. Chiu-Tsao, A. de la Zerda, J. Lin, and J. H. Kim, "High-sensitivity GafChromic film dosimetry for ¹²⁵I seed," *Med. Phys.* **21**, 651–657 (1994).
- ²³S. A. Dini, R. A. Koon, J. R. Ashburn, and A. S. Meigooni, "Dosimetric evaluation of GAFCHROMIC® XR type T and XR type R films," *J. Appl. Clin. Med. Phys.* **6**, 114–134 (2005).
- ²⁴H. Bouchard, F. Lacroix, G. Beaudoin, J.-F. Carrier, and I. Kawrakow, "On the characterization and uncertainty analysis of radiochromic film dosimetry," *Med. Phys.* **36**, 1931–1946 (2009).
- ²⁵A. Niroomand-Rad, C. R. Blackwell, B. M. Coursey, K. P. Gall, J. M. Galvin, W. L. McLaughlin, A. S. Meigooni, R. Nath, J. E. Rodgers, and C. G. Soares, "Radiochromic film dosimetry. Recommendations of AAPM Radiation Therapy Committee Task Group 55," *Med. Phys.* **25**, 2093–2115 (1998).
- ²⁶C. G. Soares, S. Trichter, and S. D. Davis, "Radiochromic film," in *Clinical Dosimetry for Radiotherapy: AAPM Summer School*, edited by D. W. O. Rogers and J. E. Cygler (Medical Physics, Madison, WI, 2009), pp. 759–813.
- ²⁷E. R. Giles and P. H. Murphy, "Measuring skin dose with radiochromic dosimetry film in the cardiac catheterization laboratory," *Health Phys.* **82**, 875–880 (2002).
- ²⁸P. Lindsay, A. Rink, M. Ruschin, and D. Jaffray, "Investigation of energy dependence of EBT and EBT-2 Gafchromic film," *Med. Phys.* **37**, 571–576 (2010).
- ²⁹B. Arjomandy, R. Taylor, N. Sahoo, M. Gillin, K. Prado, and M. Vicic, "Energy dependence and dose response of Gafchromic EBT2 film over a wide range of photon, electron, and proton beam energies," *Med. Phys.* **37**, 1942–1947 (2010).
- ³⁰S. Devic, S. Aldelajjan, H. Mohammed, N. Tomic, L.-H. Liang, F. DeBlois, and J. Seuntjens, "Absorption spectra time evolution of EBT-2 model GAFCHROMICTM film," *Med. Phys.* **37**, 2207–2214 (2010).
- ³¹O. Hupe and J. Brunzendorf, "A novel method of radiochromic film dosimetry using a color scanner," *Med. Phys.* **33**, 4085–94 (2006).
- ³²C. Richter, J. Paweike, L. Karsch, and J. Woihte, "Energy dependence of EBT-1 radiochromic film response for photon (10 kVp–15 MVp) and electron beams (6–18 MeV) readout by a flatbed scanner," *Med. Phys.* **36**, 5506–5514 (2009).
- ³³H. Alva, H. Mercado-Urbe, M. Rodríguez-Villafuerte, and M. E. Brandan, "The use of a reflective scanner to study radiochromic film response," *Phys. Med. Biol.* **47**, 2925–2933 (2002).
- ³⁴J. F. Williamson and M. J. Rivard, "Quantitative dosimetry methods for brachytherapy," in *Brachytherapy Physics: Joint AAPM/ABS Summer School*, 2nd ed., edited by B. R. Thomadsen, M. J. Rivard, and W. M. Butler (Medical Physics, Madison, WI, 2005), Monograph 31, pp. 233–294.

- ³⁵E. Yorke *et al.*, "Diode in vivo dosimetry for patients receiving external beam radiation therapy: Report of Task Group 62 of the Radiation Therapy Committee," AAPM Report No. 87 (Medical Physics Publishing, Madison, WI, 2005).
- ³⁶V. O. Zilio, O. P. Joneja, Y. Popowski, A. Rosenfeld, and R. Chawla, "Absolute depth-dose-rate measurements for an ¹⁹²Ir HDR brachytherapy source in water using MOSFET detectors," *Med. Phys.* **33**, 1532–1539 (2006).
- ³⁷R. Ramani, S. Russell, and P. O'Brien, "Clinical dosimetry using MOSFETS," *Int. J. Radiat. Oncol., Biol., Phys.* **37**, 959–964 (1997).
- ³⁸J. E. Cygler, A. Saoudi, G. Perry, C. Morash, and E. Choan, "Feasibility study of using MOSFET detectors for in vivo dosimetry during permanent low-dose-rate prostate implants," *Radiother. Oncol.* **80**, 296–301 (2006).
- ³⁹E. J. Bloemen-van Gurp, L. H. P. Murrer, B. K. C. Haanstra, F. C. J. M. van Gils, A. L. A. J. Dekker, B. J. Mijnheer, and P. Lambin, "In vivo dosimetry using a linear MOSFET-array dosimeter to determine the urethra dose in ¹²⁵I permanent prostate implants," *Int. J. Radiat. Oncol., Biol., Phys.* **73**, 314–321 (2009).
- ⁴⁰P. Karaiskos, P. Papagiannis, L. Sakelliou, G. Anagnostopoulos, and D. Baltas, "Monte Carlo dosimetry of the selectSeed ¹²⁵I interstitial brachytherapy seed," *Med. Phys.* **28**, 1753–1760 (2001).
- ⁴¹R. A. Koon, "Design and simulation of a brachytherapy source for the treatment of prostate cancer using Monte Carlo," M.S. thesis, University of Kentucky, 2005.
- ⁴²M. J. Rivard, "Monte Carlo calculations of AAPM Task Group Report No. 43 dosimetry parameters for the MED3631-A/M ¹²⁵I source," *Med. Phys.* **28**, 629–637 (2001).
- ⁴³M. J. Rivard, "Brachytherapy dosimetry parameters calculated for a ¹³¹Cs source," *Med. Phys.* **34**, 754–762 (2007).
- ⁴⁴J. Beatty, P. J. Biggs, K. Gall, P. Okunieff, F. S. Pardo, K. J. Harte, M. J. Dalterio, and A. P. Sliiski, "A new miniature x-ray source for interstitial radiosurgery: Dosimetry," *Med. Phys.* **23**, 53–62 (1996).
- ⁴⁵M. J. Rivard, S. D. Davis, L. A. DeWerd, T. W. Rusch, and S. Axelrod, "Calculated and measured brachytherapy dosimetry parameters in water for the Xofigo x-ray source: An electronic brachytherapy source," *Med. Phys.* **33**, 4020–4032 (2006).
- ⁴⁶A. S. Meigooni, H. Zhang, J. R. Clark, V. Rachabathula, and R. A. Koon, "Dosimetric characteristics of the new RadioCoil™ ¹⁰³Pd wire line source for use in permanent brachytherapy implants," *Med. Phys.* **31**, 3095–3105 (2004).
- ⁴⁷M. J. Rivard, D. Granero, J. Perez-Calatayud, and F. Ballester, "Influence of photon energy spectra from brachytherapy sources on Monte Carlo simulations of kerma and dose rates in water and air," *Med. Phys.* **37**, 869–876 (2010).
- ⁴⁸D. Baltas, P. Karaiskos, P. Papagiannis, L. Sakelliou, E. Löffler, and N. Zamboglou, "Beta versus gamma dosimetry close to Ir-192 brachytherapy sources," *Med. Phys.* **28**, 1875–1882 (2001).
- ⁴⁹R. Wang and X. A. Li, "Dose characterization in the near-source region for two high dose rate brachytherapy sources," *Med. Phys.* **29**, 1678–1686 (2002).
- ⁵⁰F. Ballester, D. Granero, J. Perez-Calatayud, C. S. Melhus, and M. J. Rivard, "Evaluation of high-energy brachytherapy source electronic disequilibrium and dose from emitted electrons," *Med. Phys.* **36**, 4250–4256 (2009).
- ⁵¹NUDAT 2.5, National Nuclear Data Center, Brookhaven National Laboratory, Upton, NY, USA, <http://www.nndc.bnl.gov/nudat2/index.jsp> (last accessed December 5, 2010).
- ⁵²J. Pérez-Calatayud, D. Granero, and F. Ballester, "Phantom size in brachytherapy source dosimetric studies," *Med. Phys.* **31**, 2075–2081 (2004).
- ⁵³C. S. Melhus and M. J. Rivard, "Approaches to calculating AAPM TG-43 brachytherapy dosimetry parameters for ¹³⁷Cs, ¹²⁵I, ¹⁹²Ir, ¹⁰³Pd, and ¹⁶⁹Yb sources," *Med. Phys.* **33**, 1729–1737 (2006).
- ⁵⁴R. E. P. Taylor and D. W. O. Rogers, "An EGSnrc Monte Carlo-calculated database of TG-43 parameters," *Med. Phys.* **35**, 4228–4241 (2008).
- ⁵⁵A. S. Meigooni, S. B. Awan, N. S. Thompson, and S. A. Dini, "Updated Solid Water™ to water conversion factors for ¹²⁵I and ¹⁰³Pd brachytherapy sources," *Med. Phys.* **33**, 3988–3992 (2006).
- ⁵⁶N. S. Patel, S.-T. Chiu-Tsao, J. F. Williamson, P. Fan, T. Duckworth, D. Shasha, and L. B. Harrison, "Thermoluminescent dosimetry of the Symmetra™ ¹²⁵I model I25.S06 interstitial brachytherapy seed," *Med. Phys.* **28**, 1761–1769 (2001).
- ⁵⁷R. E. P. Taylor and D. W. O. Rogers, "EGSnrc Monte Carlo calculated dosimetry parameters for ¹⁹²Ir and ¹⁶⁹Yb brachytherapy sources," *Med. Phys.* **35**, 4933–4944 (2008).
- ⁵⁸J. J. DeMarco, R. E. Wallace, and K. Boedeker, "An analysis of MCNP cross-sections and tally methods for low-energy photon emitters," *Phys. Med. Biol.* **47**, 1321–1332 (2002).
- ⁵⁹D. E. Cullen, J. H. Hubbell, and L. Kissel, "EPDL97: The Evaluated Photon Data Library, '97 Version," Lawrence Livermore National Laboratory Report No. UCRL-50400, Vol. 6, Rev. 5 (19 September 1997).
- ⁶⁰S. M. Seltzer, "Calculation of photon mass energy-transfer and mass energy-absorption coefficients," *Radiat. Res.* **136**, 147–170 (1993).
- ⁶¹J. F. Williamson, "Monte Carlo evaluation of kerma at a point for photon transport problems," *Med. Phys.* **14**, 567–576 (1987).
- ⁶²M. J. Rivard, C. S. Melhus, D. Granero, J. Perez-Calatayud, and F. Ballester, "An approach to using conventional brachytherapy software for clinical treatment planning of complex, Monte Carlo-based brachytherapy dose distributions," *Med. Phys.* **36**, 1968–1975 (2009).
- ⁶³S. M. Seltzer, P. J. Lamperti, R. Loevinger, M. G. Mitch, J. T. Weaver, and B. M. Coursey, "New national air-kerma-strength standards of I-125 and Pd-103 brachytherapy seeds," *J. Res. Natl. Inst. Stand. Technol.* **108**, 337–358 (2003).
- ⁶⁴M. G. Mitch and C. G. Soares, "Primary standards for brachytherapy sources," in *Clinical Dosimetry for Radiotherapy: AAPM Summer School*, edited by D. W. O. Rogers and J. E. Cygler (Medical Physics, Madison, WI, 2009), pp. 549–565.
- ⁶⁵C. G. Soares, G. Douysset, and M. G. Mitch, "Primary standards and dosimetry protocols for brachytherapy sources," *Metrologia* **46**, S80–S98 (2009).
- ⁶⁶H.-J. Selbach, H.-M. Kramer, and W. S. Culbertson, "Realization of reference air-kerma rate for low-energy photon sources," *Metrologia* **45**, 422–428 (2008).
- ⁶⁷T. P. Loftus, "Standardization of iridium-192 gamma-ray sources in terms of exposure," *J. Res. Natl. Bur. Stand.* **85**, 19–25 (1980).
- ⁶⁸Z. Li, R. K. Das, L. A. DeWerd, G. S. Ibbott, A. S. Meigooni, J. Perez-Calatayud, M. J. Rivard, R. S. Sloboda, and J. F. Williamson, "Dosimetric prerequisites for routine clinical use of photon emitting brachytherapy sources with average energy higher than 50 keV," *Med. Phys.* **34**, 37–40 (2007).
- ⁶⁹T. P. Loftus, "Standardization of cesium-137 gamma-ray sources in terms of exposure units (Roentgens)," *J. Res. Natl. Bur. Stand., Sect. A* **74A**, 1–6 (1970).
- ⁷⁰R. Nath, L. L. Anderson, J. A. Meli, A. J. Olch, J. A. Stitt, and J. F. Williamson, "Code of practice for brachytherapy physics: Report of the AAPM Radiation Therapy Committee Task Group No. 56," *Med. Phys.* **24**, 1557–1598 (1997).
- ⁷¹S. J. Goetsch, F. H. Attix, D. W. Pearson, and B. R. Thomadsen, "Calibration of ¹⁹²Ir high-dose-rate afterloading systems," *Med. Phys.* **18**, 462–467 (1991).
- ⁷²E. Mainegra-Hing and D. W. O. Rogers, "On the accuracy of techniques for obtaining the calibration coefficient NK of ¹⁹²Ir HDR brachytherapy sources," *Med. Phys.* **33**, 3340–3347 (2006).
- ⁷³E. van Dijk, I.-K. K. Kolkman-Deurloo, and P. M. G. Damen, "Determination of the reference air kerma rate for ¹⁹²Ir brachytherapy sources and the related uncertainty," *Med. Phys.* **31**, 2826–2833 (2004).
- ⁷⁴K. E. Stump, L. A. DeWerd, J. A. Micka, and D. R. Anderson, "Calibration of new high dose rate ¹⁹²Ir sources," *Med. Phys.* **29**, 1483–1488 (2002).
- ⁷⁵A. M. Bidmead, T. Sander, S. M. Locks, C. D. Lee, E. G. A. Aird, R. F. Nutbrown, and A. Flynn, "The IPeM code of practice for determination of the reference air kerma rate for HDR ¹⁹²Ir brachytherapy sources based on the NPL air kerma standard," *Phys. Med. Biol.* **55**, 3145–3159 (2010).
- ⁷⁶G. Douysset, J. Gouriou, F. Delaunay, L. DeWerd, K. Stump, and J. Micka, "Comparison of dosimetric standards of USA and France for HDR brachytherapy," *Phys. Med. Biol.* **50**, 1961–1978 (2005).
- ⁷⁷G. Douysset, T. Sander, J. Gouriou, and R. Nutbrown, "Comparison of air kerma standards of LNE-LNHB and NPL for ¹⁹²Ir HDR brachytherapy sources: EUROMET Project No 814," *Phys. Med. Biol.* **53**, N85–N97 (2008).
- ⁷⁸L. A. DeWerd, M. S. Huq, I. J. Das, G. S. Ibbott, W. F. Hanson, T. W. Slowey, J. F. Williamson, and B. M. Coursey, "Procedures for establishing and maintaining consistent air-kerma strength standards for low-energy, photon-emitting brachytherapy sources: Recommendations of the Calibration Laboratory Accreditation Subcommittee of the American As-

- sociation of Physicists in Medicine,” *Med. Phys.* **31**, 675–681 (2004).
- ⁷⁹W. M. Butler, W. S. Bice, Jr., L. A. DeWerd, J. M. Hevezi, M. S. Huq, G. S. Ibbott, J. R. Palta, M. J. Rivard, J. P. Seuntjens, and B. R. Thomadsen, “Third-party brachytherapy source calibrations and physicist responsibilities: Report of the AAPM Low Energy Brachytherapy Source Calibration Working Group,” *Med. Phys.* **35**, 3860–3865 (2008).
- ⁸⁰J. A. Meli, “Let’s abandon geometry factors other than that of a point source in brachytherapy dosimetry,” *Med. Phys.* **29**, 1917–1918 (2002).
- ⁸¹M. J. Rivard, B. M. Coursey, L. A. DeWerd, W. F. Hanson, M. S. Huq, G. Ibbott, R. Nath, and J. F. Williamson, “Comment on ‘Let’s abandon geometry factors other than that of a point source in brachytherapy dosimetry’ [Med Phys. **29**, 1917–1918 (2002)],” *Med. Phys.* **29**, 1919–1920 (2002).
- ⁸²M. J. Rivard, L. Beaulieu, and F. Mourtada, “Necessary enhancements to commissioning techniques of brachytherapy treatment planning systems that use model-based dose calculation algorithms,” *Med. Phys.* **37**, 2645–2658 (2010).
- ⁸³S. Nag, R. Dobelbower, G. Glasgow, G. Gustafson, N. Syed, B. Thomadsen, and J. F. Williamson, “Inter-society standards for the performance of brachytherapy: A joint report from ABS, ACMP and ACRO,” *Crit. Rev. Oncol. Hematol.* **48**, 1–17 (2003).
- ⁸⁴F. Ballester, D. Granero, J. Perez-Calatayud, J. L. M. Venselaar, and M. J. Rivard, “Study of encapsulated ^{170}Tm sources for their potential use in brachytherapy,” *Med. Phys.* **37**, 1629–1637 (2010).